A RECIPROCAL FERRITE PHASE SHIFTER FOR X-BAND

A Thesis

Presented To

the Faculty of Graduate Studies and Research

The University of Manitoba

In Partial Fulfillment

of the Requirements for the Degree

Master of Science in Electrical Engineering

---

by

Barry Arthur Gordon

October 1964

ABSTRACT

It was the purpose of this study to investigate the characteristics of a magnetically controlled microwave phase shifter and to determine the useful bandwidth of such a device.

PREFACE

The objective of this thesis was to construct a magnetically controlled ferrite phase shifter suitable for installation in X-band rectangular waveguide, and to determine experimentally the phase shift characteristics and operational limitations of this device.

To familiarize the reader with the basic electromagnetic properties of ferrite materials, a resume of their significant characteristics is given in an introductory chapter. In succeeding chapters, the phase shift properties of the device are presented for two matching systems, accompanied by an account of loss effects and standing wave ratio. Quantitative evaluation of the errors inherent in the phase measuring technique is also done at this point. An attempt is then made to explain the operation of the device and to predict quantitative values of phase shift by comparison of this assembly with an unbounded isotropic dielectric rod waveguide.

I wish to acknowledge the assistance and guidance given me by Professor E. Bridges, and also the encouragement and help of my wife.

TABLE OF CONTENTS

TABLE OF CONTENTS (continued)

LIST OF GRAPHS

LIST OF GRAPHS (continued)

LIST OF FIGURES

LIST OF TABLES

CHAPTER I

INTRODUCTION TO MICROWAVE FERRITES

1.1 Background

The theory of microwave ferrites has received considerable attention in recent years and many investigators have made notable contributions. The study of ferrite loaded waveguides centres on the solution of Maxwell's field equations subject to the appropriate boundary conditions. Unfortunately, only two waveguide-ferrite geometries have proven amenable to exact solution and consequently many useful configurations have had to be analyzed by means of perturbational technique or through identification with similar structures that are subject to exact mathematical description.

The first configuration to be analyzed exactly was the case of a cylindrical ferrite rod, magnetised axially, completely or partially filling a section of cylindrical waveguide. This case has been thoroughly investigated by Kales[1], Suhl and Walker[2], and others.[3,4] Practical devices utilizing this geometry are the Faraday rotation isolator[5], amplitude modulator[6], and circulator.[7]

The case of a section of rectangular waveguide loaded with a ferrite slab, magnetised transversely, has received

---

[1] See bibliography, Ref. #1. Superscripts, henceforth, will refer to numbered references in the bibliography.

thorough treatment by a number of investigators.[8,9] Useful devices arising from these studies include reciprocal and nonreciprocal phase shifters,[10] resonance isolators,[4] field displacement isolators[9] and circulators.[11]

Since the geometry dealt with in this thesis involves a round ferrite rod mounted in a rectangular waveguide and magnetised parallel to the direction of propagation, insight into its behavior will have to be gained through comparison with an unbounded dielectric rod waveguide.

1.2 Ferrite Crystal Chemistry

Ferrites are ceramic ferromagnetic materials with the general chemical composition $MO.Fe_2O_3$ where M is a divalent metal such as iron, manganese, magnesium, nickel, zinc, cadmium, cobalt, copper, aluminum, or a mixture of these. Compounds with this general formula contain unpaired electrons and thus exhibit ferromagnetism.

1.3 General Physical Properties

If stoichiometric properties are maintained, ferrite materials are non-conductors. Departures from the ideal chemical formula or crystal structure in preparation create free electrons and/or holes and the ferrite becomes a semi-conductor. Typical values for the resistivity of commercially available ferrites are 10^2 to 10^6 ohm-meters. Resistive losses in the ferrite material are therefore small.

The permittivity of ferrite materials at X-band frequencies is usually of the order of 10 to 20 times the permittivity of free space. This permittivity is complex, but the imaginary component is generally small and consequently dielectric losses are low.

The permeability of ferrite materials is characterized in the general case by a tensor of the following form.[12,13]

$$\begin{bmatrix} B_x \\ B_y \\ B_z \end{bmatrix} = \mu_0 \begin{bmatrix} \mu & -j\alpha & 0 \\ j\alpha & \mu & 0 \\ 0 & 0 & 1 \end{bmatrix} \cdot \begin{bmatrix} H_x \\ H_y \\ H_z \end{bmatrix}$$

Where B_i and H_i represent the microwave field inside the ferrite specimen and the expressions for μ and α are:

$$\mu = 1 + \frac{\mu_0 \gamma^2 H_0 M_s}{\gamma^2 \mu_0^2 H_0^2 - \omega^2}$$

$$\alpha = \frac{\gamma M_s \omega}{\gamma^2 \mu_0^2 H_0^2 - \omega^2}$$

where μ_0 - permeability of free space
γ - gyromagnetic ratio (2.8 Mc./s./oersted)
ω - operating angular frequency
M_s - saturation magnetisation of the ferrite
H_0 - direct magnetising field inside the ferrite specimen applied in the Z direction

The above expression for the components of the permeability tensor are theoretical and apply to an ideal lossless case at magnetic saturation. The variations of the components with applied field for a typical ferrite are shown in figure 1 in appendix I. With zero applied field

the ferrite is seen to degenerate to an isotropic dielectric. As the applied field (H_o) is increased from zero a point is approached (for a given value of ω) where gyromagnetic resonance occurs. The phenomenon of gyromagnetic resonance results when $\omega = \gamma\mu_r H_o$ and both μ_r and κ become infinite in the ideal lossless case.

In practice the components of the permeability tensor are complex and there is some magnetic loss due to relaxation effects. The imaginary parts of μ_r and κ (and consequently the loss) are, however, negligible below gyromagnetic resonance. In practical ferrites also, μ_r and κ do not become infinite at gyromagnetic resonance but do become very large.

In this study applied field strengths (H_o) are restricted to values far below the resonance value and therefore magnetic losses remain insignificant. (Actually to obtain resonance at X-band frequencies, a field of greater than 2000 oersteds is required. The greatest field strength achieved in this work was approximately 180 oersteds.)

For a thorough discussion of the permeability tensor and its derivation, the reader is referred to the literature.[12,13]

CHAPTER II

EXPERIMENTAL PROCEDURE

A schematic of the basic equipment layout for the experimental work described in the succeeding three sections is given in figure 2.1. Also provided is a photograph (figure 2.2) of the general experimental setup.

2.1 Measurement of Phase Shift

Any matched section of waveguide will produce a characteristic phase shift per unit length that is frequency dependent. In this study, the unmagnetised phase shift of the device was chosen as the zero phase shift reference. The term "phase shift", as used in this thesis, will then mean the increase in phase shift over the phase shift of the unmagnetised device.

The phase shift through the ferrite loaded section of waveguide was measured by the adjustable short method described by Magid.[14] This method is applicable to reciprocal devices only, since the phase shift is assumed to be the same regardless of the direction of propagation.

The probe of the standing wave detector was positioned at a reference minimum. As the phase shift was increased, by increasing the coil current, the reference minimum migrated towards the load. This direction of minimum shaft indicated

that the change in phase shift through the device was actually an increase in phase retardation. The short was adjusted to return the reference minimum to its original position. Since the wave travelled through the component in both directions (being perfectly reflected by the short circuit), twice the phase shift of the device is equal to the change in phase of the reflection coefficient (from its initial reference value) of the adjustable short circuit. Mathematically, this relation is:

$$\phi = \frac{360^{\circ}\Delta x}{\lambda_g}$$

where ϕ - phase shift (Degrees)
Δx - change in setting of adjustable short
λ_g - guide wavelength

For selected frequencies, the phase shift at a number of coil current settings up to saturation was measured.

2.2 Measurement of the Standing Wave Ratio

The standing wave ratio of the device was measured by terminating the output port with a matched load. In this configuration, all reflections were due to the device itself.

2.3 Measurement of Insertion Loss

The insertion loss of the ferrite loaded section was determined by the attenuation substitution method.

The incident power to the device was measured via the directional coupler. The output power of the device was noted

and recorded. The device was then removed and replaced by a continuously variable precision attenuator.

The attenuator was adjusted to produce the same output power as previously recorded, with the incident power unchanged. The setting of the attenuator was then taken as the characteristic insertion loss of the ferrite loaded section of waveguide.

It should be noted that this method does not distinguish between reflective losses and dissipative losses in the ferrite itself.

2.4 Sources of Experimental Error

Inherent in the phase measuring technique utilized in this thesis is an error in measured phase, due to imperfect matching of the ferrite loaded section to the preceeding empty waveguide. This error is evaluated quantitatively in the next chapter. The origin of this error and the derivation of the formula for its calculation is outlined in appendix II.

Compared with the above error, other errors in phase measurement due to the limit of accuracy to which the position of the adjustable short, the coil current, the frequency or the guide wavelength can be read, are negligible. There is another possible error in phase shift results due to carelessness in the centralization of the ferrite rod within the waveguide. Discussion of this error is done in the next chapter.

Experimental errors in the measurement of VSWR or loss are almost nonexistent. A slight VSWR error could result due to probe loading but the magnitude of such an error is undoubtedly small since the probe penetration was always reduced to a minimum.

All experimental results could exhibit a certain degree of inaccuracy due to the equipment and meters being out of calibration, but quantitative analysis of errors of this type is impossible.

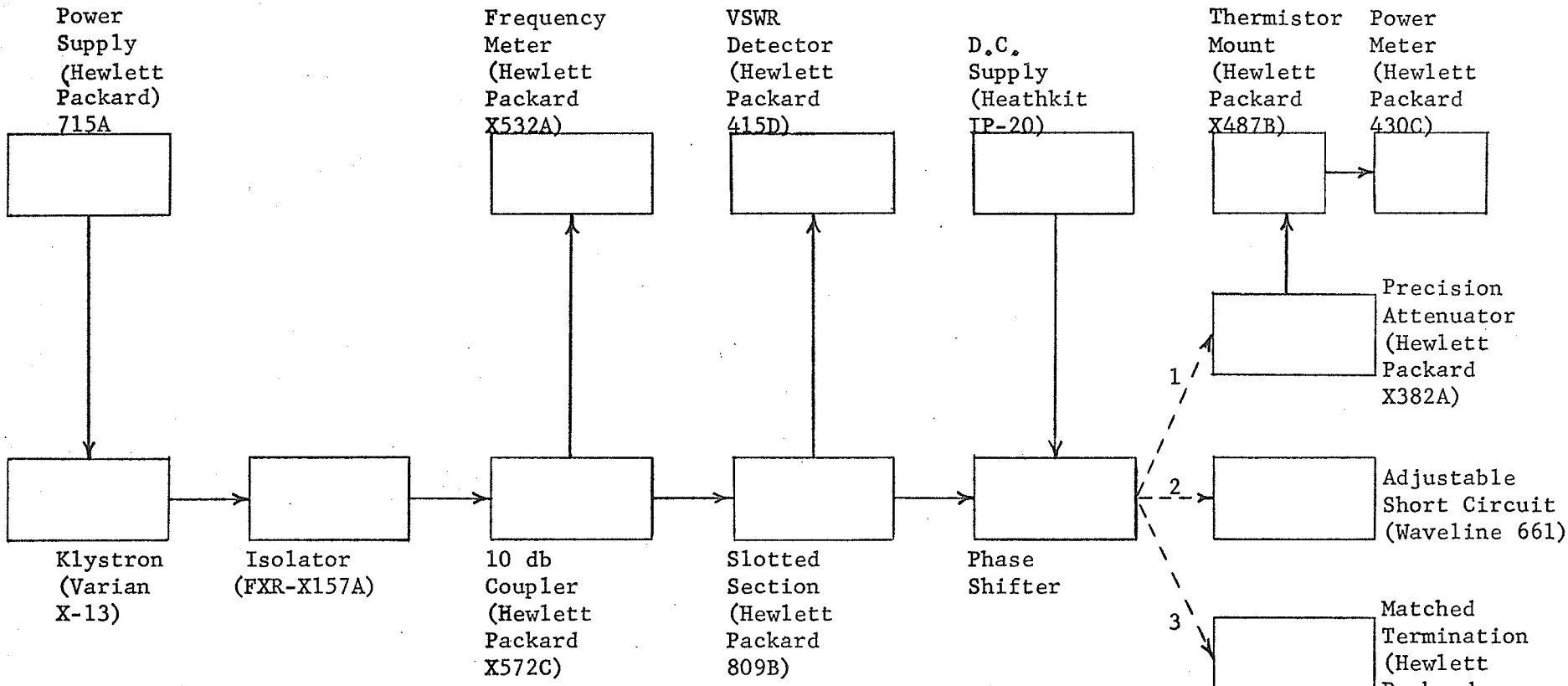

Position: 1. Insertion loss measurement.
2. Phase shift measurement.
3. VSWR measurement.

Figure 2.1
Basic Equipment Layout

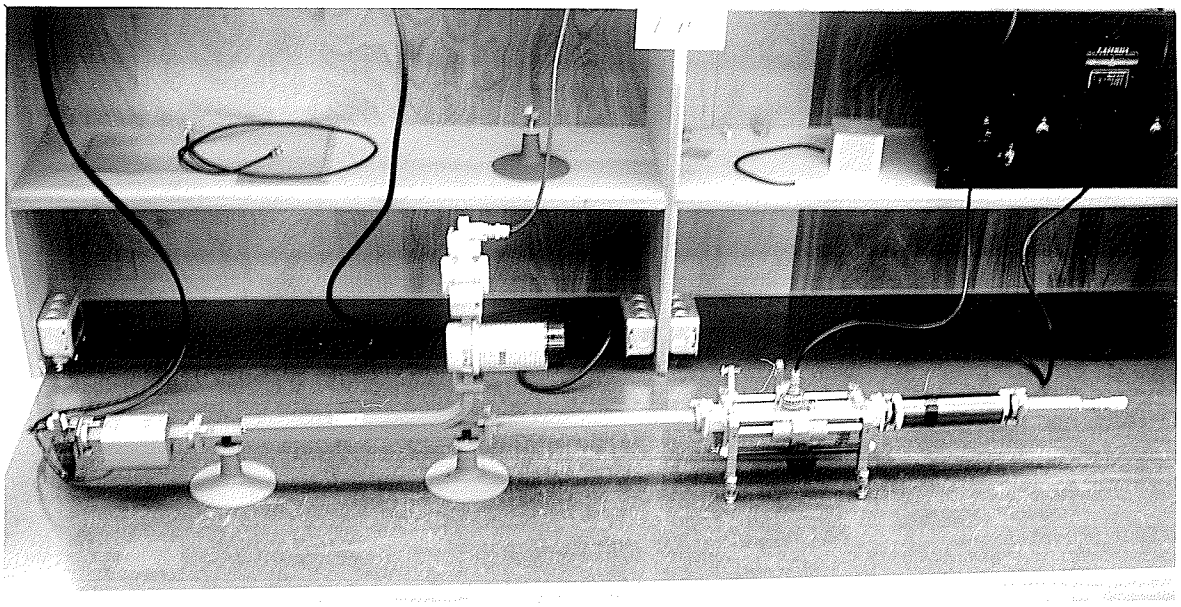

Figure 2.2

Basic Equipment Layout

CHAPTER III

THE FERRITE PHASE SHIFTER

3.1 Description of the Phase Shifting Assembly

The phase shifting assembly constructed and tested in this study was similar to the device described by Reggia and Spencer.[15] The device consisted of a ferrite rod 2 inches long and 0.25 inches in diameter, supported centrally inside a section of rectangular waveguide by polyurethane (ϵ=1.01) supports. On either end of the ferrite rod were mounted impedance-matching tips and around the exterior of the rectangular waveguide was wound a current solenoid. A diagram of the ferrite assembly and the solenoid is shown in figure 3.1. A photograph of the constituent parts of the device is given in figure 3.2.

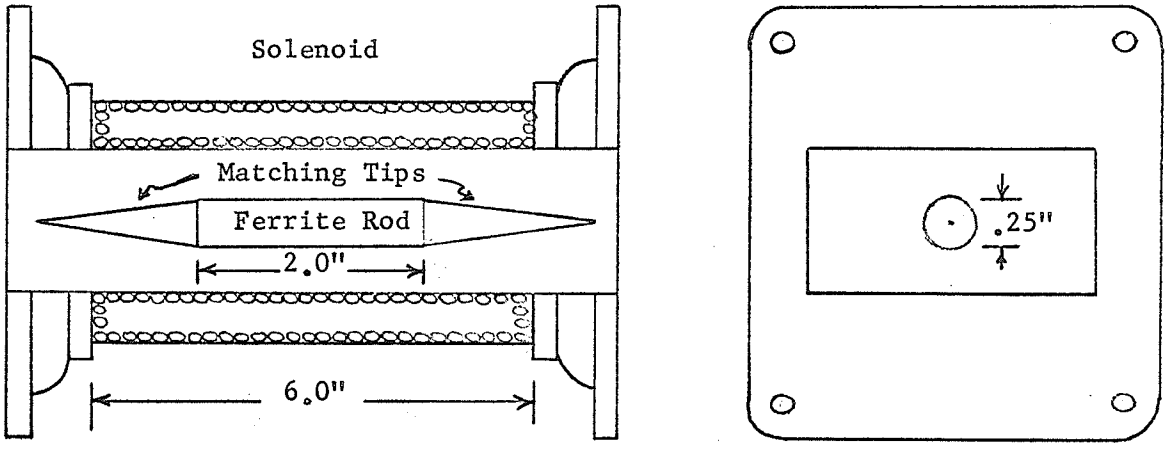

Figure 3.1

Phase Shifter Assembly and Solenoid

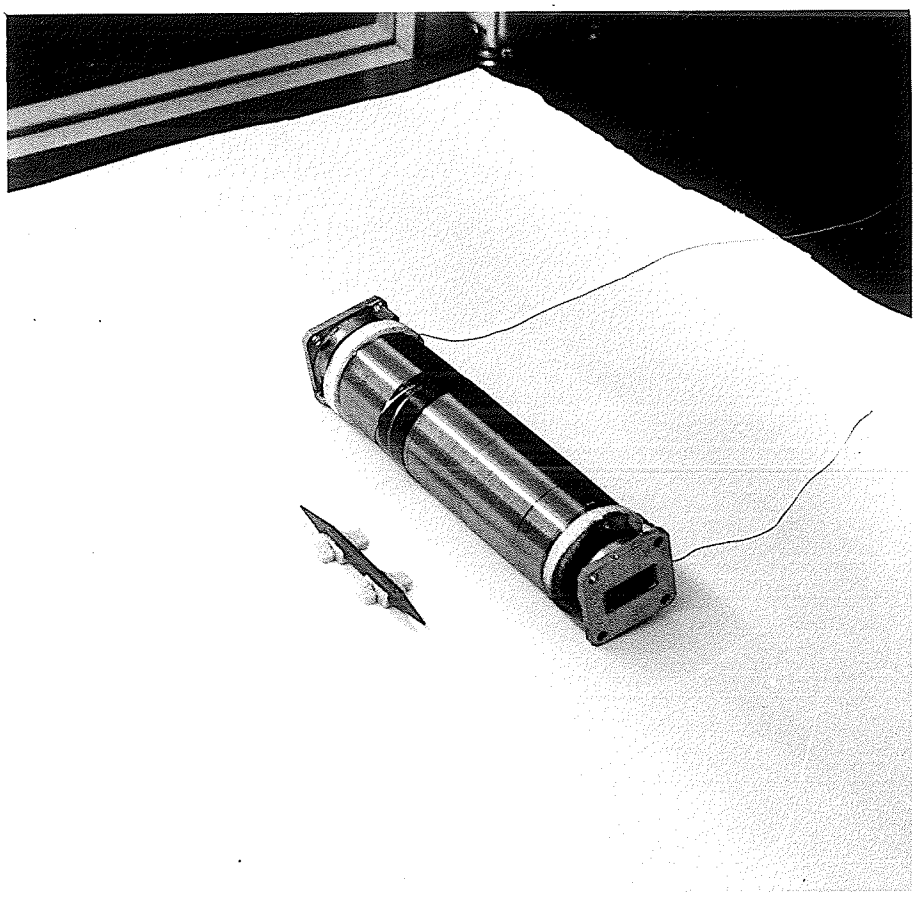

Figure 3.2

Phase Shifter Assembly and Solenoid

The ferrite used was a low loss MgMn material available commercially as Ferramic R-1. The electromagnetic properties of this material are summarized in Appendix I.

The solenoid supplying the longitudinal magnetic field consisted of approximately 1400 turns of #24 enamelled copper wire wound around a six inch length of the rectangular waveguide. The D. C. resistance of the solenoid was 15 ohms. The magnetic field sensitivity was nominally 120 oersteds/ampere with the ferrite rod removed. Since it requires approximately 150 oersteds to saturate the ferrite,[21] a coil current of 1.3 amperes was assumed sufficient to produce saturation. (The demagnetising factor of a long thin rod magnetised axially is zero,[23] the D. C. applied field in the centre of the waveguide is therefore essentially the same with or without the ferrite present.)

The initial phase shifter assembly was constructed using phenol ($\epsilon = 4.5$) matching tips, 1.875 inches long and tapered to a point. In an attempt to improve the match between the empty waveguide and the ferrite loaded section, a second assembly was built using tapered ferrite tips. These tips were one inch long.

3.2 Experimental Results - Phenol Matching Tips

The first measurements made were those of VSWR and insertion loss of the phase shifter at zero magnetisation and then at saturation magnetisation. Measurements were made at

frequencies in the X-band and the results are shown in graph 3.1. It is seen from this graph that for both magnetisation states there exists a frequency above which both the loss and VSWR exhibit large fluctuations. (Approximately 10.8 Gc. for the unmagnetised case and 10.0 Gc. for the saturated case.) These variations are due to the existence of higher order modes on the ferrite structure. The ability of the structure to support these modes will be disucssed in the next chapter. Since it is impossible to produce an impedance match for two or more modes propagating simultaneously, the first operational limit of the device is encountered. The upper frequency limit was taken as the frequency above which higher order modes existed in the saturated device. From graph 3.1, this frequency is seen to be approximately 10 Gc.

Another interesting feature of the VSWR and insertion loss curves of graph 3.1, is that the curve of insertion loss follows the curve of VSWR (with one exception). The primary source of loss in the device is therefore due to input reflections. The exception occurs at a frequency of 8.84 Gc. in the unmagnetised case. There is no peak in the VSWR curve corresponding to the loss peak, and therefore the loss must be due to dissipation in the ferrite. No reasonable explanation for the size or position of this loss peak exists.

The next step in the testing of the device was to measure the phase shift, VSWR and insertion loss at frequencies of 8.55

Gc., 9.014 Gc., 9.390 Gc., 9.747 Gc. and 10.106 Gc., with coil currents increasing from zero to 1.3 amperes (effective saturation). The results of these measurements are displayed on graphs 3.2 to 3.6 inclusively. Also plotted on these graphs are curves of maximum phase error due to reflections from the ferrite loaded section. The theoretical derivation of this error and the formula for its calculation are given in Appendix II.

Since the phase measuring method involved in this work was based on the premise that the phase shift through the device was reciprocal, the results stated herein are meaningless unless the phase shifts were, in fact, reciprocal. It has been stated in the literature that a ferrite rod positioned centrally inside a section of rectangular waveguide will produce reciprocal phase shifts.[15] The greatest precautions were taken at all times to ensure that the ferrite rod was indeed centred and hence the results may be taken as being accurate in this regard.

The reciprocity of the VSWR and insertion loss of device was checked by physically exchanging the coil and rod assembly end for end and remeasuring the VSWR and loss. At all frequencies and current settings the VSWR and insertion loss were seen to be identical regardless of the direction of propagation. (This provides more assurance that the phase shift was also reciprocal, since nonreciprocal phase shifts would undoubtedly manifest themselves in the VSWR and insertion loss results.)

The curves of phase shift vs. coil shift at all frequencies have a common shape. The maximum phase slope occurred in the coil current range from 0 to 400 ma. Above 400 ma. the slope decreased as the ferrite began to saturate. It is believed that the curves would exhibit greater flattening at high coil currents if it weren't for the heating of the ferrite due to the D. C. power dissipated in the coil. At a coil current of one ampere, the coil must dissipate 15 watts. Since the field required to saturate the ferrite increases with temperature, this offsets the tendency to saturate at higher coil currents. The characteristic shape of the phase shift curves is remarkably similar to the curve for the variation of μ with field intensity (Figure 1, Appendix I). In the succeeding chapter this variation of μ will be shown to be the dominant factor producing the phase shift and hence the similarity.

The effect of hysterisis can be seen by referring to graph 3.3. Since the phase difference due to hysterisis was overshadowed in all cases by the maximum possible error in phase due to measurement technique, very little significance can be given to quanitative hysterisis information. Its existence is, however, confirmed.

At all test frequencies, the loss vs. current curve has the same general shape as the VSWR curve. This agreement of curve shape emphasizes the fact that the insertion loss is

due primarily to input reflections and very little energy is dissipated in the ferrite itself.

The saturation phase shift was found to be a function of the frequency and reference to graph 3.7 indicates that the relationship is linear.

A summary of the significant properties of the device at each test frequency is given in table 3.1.

Frequency (Gc./s.)	Sat. Phase Shift	VSWR	Loss (db)
8.555	110°	1.15±.15	1.20±.10
9.014	230°	1.30±.30	1.50±.30
9.390	300°	1.35±.30	1.35±.20
9.747	400°	1.50±.45	1.60±.35
10.106	480°	1.60±.50	1.90±.40

Table 3.1

Phase Shifter Properties - Phenol Matching Tips

As was noted previously, the ferrite structure was able to support higher order modes above a frequency of 10.0 Gc./s. Another consequence of the existence of these higher order modes at frequencies above 10.0 Gc./s. is that large reciprocal phase shifts are no longer readily available. At these frequencies, the energy is concentrated principally in the ferrite rod. The rectangular waveguide walls have lost their dominant role in the guiding of the microwave fields. Examination of the permeability tensor on page 3 shows that there

is a coupling of some of the energy of the vertically polarised TE_{10} mode into horizontally polarised energy. This coupling is due to the off-diagonal component α. It can be shown that the velocities of propagation of the horizontally polarised component and the vertically polarised component are not the same. Thus the resultant electric field vector will be linearly polarised at any instant but the plane of linear polarisation will rotate as the fields propagate along the rod. This is the phenomenon of Faraday rotation. Since the rectangular walls are not "seen" by the microwave fields they can no longer suppress this rotation. Hence, the coupling to the succeeding empty waveguide is a function of the angle of polarisation at the output of the ferrite rod. Referring to figure 3.2, it is noted that when θ is $\frac{n\pi}{2}$ (n = 1,3,5, etc.), the coupling will be a maximum.

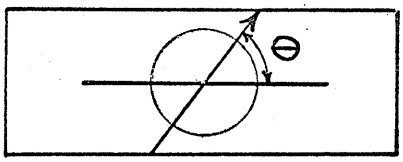

Figure 3.3

Faraday Rotation of the Plane of Polarisation

When n is an even integer, the coupling to the dominant TE_{10} mode will be a minimum and the insertion loss will be a maximum. The results of a loss test at a frequency of 11.120 Gc./s.

are displayed on graph 3.8. The values of Θ at the peaks and troughs of the curve are given. It must be borne in mind that the large phase shifts are still present, but the variations in transmitted power render the device pratically unusable as a phase shifter.

3.3 Experimental Results - Ferrite Matching Tips

The phenol matching tips of the previous section were replaced by ferrite tips in an attempt to realize lower VSWR's over the usable frequency range of the device.

As before, the first tests made were of VSWR and insertion loss at zero and then at saturation magnetisation at selected frequencies. Since the addition of ferrite tips will have no effect on the propagation of higher order modes, the tests were conducted over the useful frequency range of the device only (8.2 Gc./s. - 10.0 Gc./s.). The results of the tests are given in graph 3.9.

Reference to graph 3.9 and to graph 3.1 indicates that no improvement in VSWR has been realized in the zero magnetisation case. There is, however, a slight improvement in the VSWR of the saturation magnetisation case. It is interesting to observe that the anomalous loss peak at 8.8 Gc./s. is still present. A summary of the median VSWR's and the limits of variation in the frequency range from 8.2 - 10.0 Gc./s. for the two matching systems is given in table 3.2.

VSWR

	Phenol Tips	Ferrite Tips
Zero Magnetisation	1.3±.3	1.5±.5
Sat. Magnetisation	1.5±.3	1.3±.3

Table 3.2

Comparison of the VSWR's for Phenol & Ferrite Matching Tips

Phase shift, VSWR, and insertion loss measurements at increasing magnetisation levels were made for the same test frequencies listed in section 3.2. The results of these measurements are displayed on graphs 3.10 to 3.14 inclusively. Again curves of maximum phase error accompany the phase shift curves.

As with the previous results for the case of phenol matching tips, the phase shift curves for all test frequencies exhibit a common shape and the same comments that were made in section 3.2 still apply.

Reference to graphs 3.10 to 3.14, reveals that the loss is somewhat less than with phenol matching tips. This is not considered significant because failure to reproduce the exact test frequencies of section 3.2 in this section makes comparison difficult.

The saturation phase was again found to be a linear function of frequency (see graph 3.15). The saturation phase shift is, however, larger than that produced by the previous

configuration at any given frequency. This is due to the addition of the ferrite tips which aid in the production of phase shift under magnetisation. Assuming that the 1" ferrite tips are perfect cones 0.125" in base radius, then the total ferrite volume in the cones is 0.324 cubic inches. The length of an equivalent cylinder 0.125" in radius is, therefore, 0.66 inches. Hence the total equivalent rod length producing phase shift is 2.66 inches. Graph 3.16 displays the saturation phase shift at the test frequencies for both matching systems normalized to a one inch rod length. It is seen from this data that there is excellent agreement between the results produced by the phase shifter with both matching systems.

A summary of the characteristics of the ferrite tipped phase shifter is given in table 3.3.

Frequency (Gc./s.)	Sat. Phase Shift	VSWR	Loss (db)
8.558	146°	1.20±.20	0.6±0.10
9.005	282°	1.18±.12	0.6±0.10
9.392	406°	1.27±.25	1.17±0.75
9.748	525°	1.19±.16	0.6±0.20
10.107	600°	1.26±.20	1.9±1.20

Table 3.3

Phase Shifter Properties - Ferrite Matching Tips

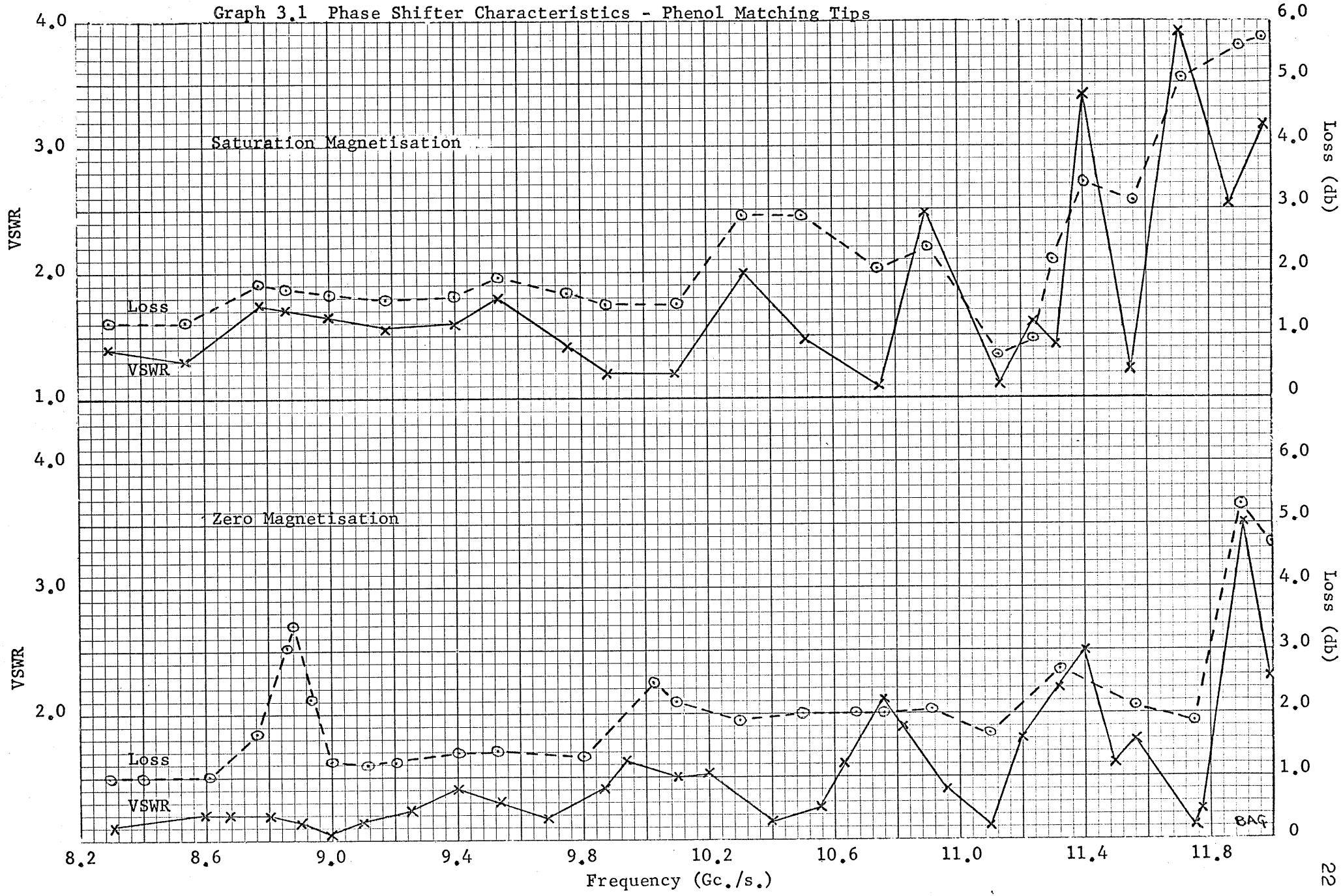
Graph 3.1 Phase Shifter Characteristics - Phenol Matching Tips
Saturation Magnetisation
Zero Magnetisation
Loss
VSWR
Loss
VSWR
VSWR
Loss (db)
VSWR
Loss (db)
4.0
3.0
2.0
1.0
6.0
5.0
4.0
3.0
2.0
1.0
0
8.2
8.6
9.0
9.4
9.8
10.2
10.6
11.0
11.4
11.8
Frequency (Gc./s.)
BAG

Graph 3.2
Ferrite Phase Shifter - Phenol Matching Tips Frequency 8.555 Gc./s.

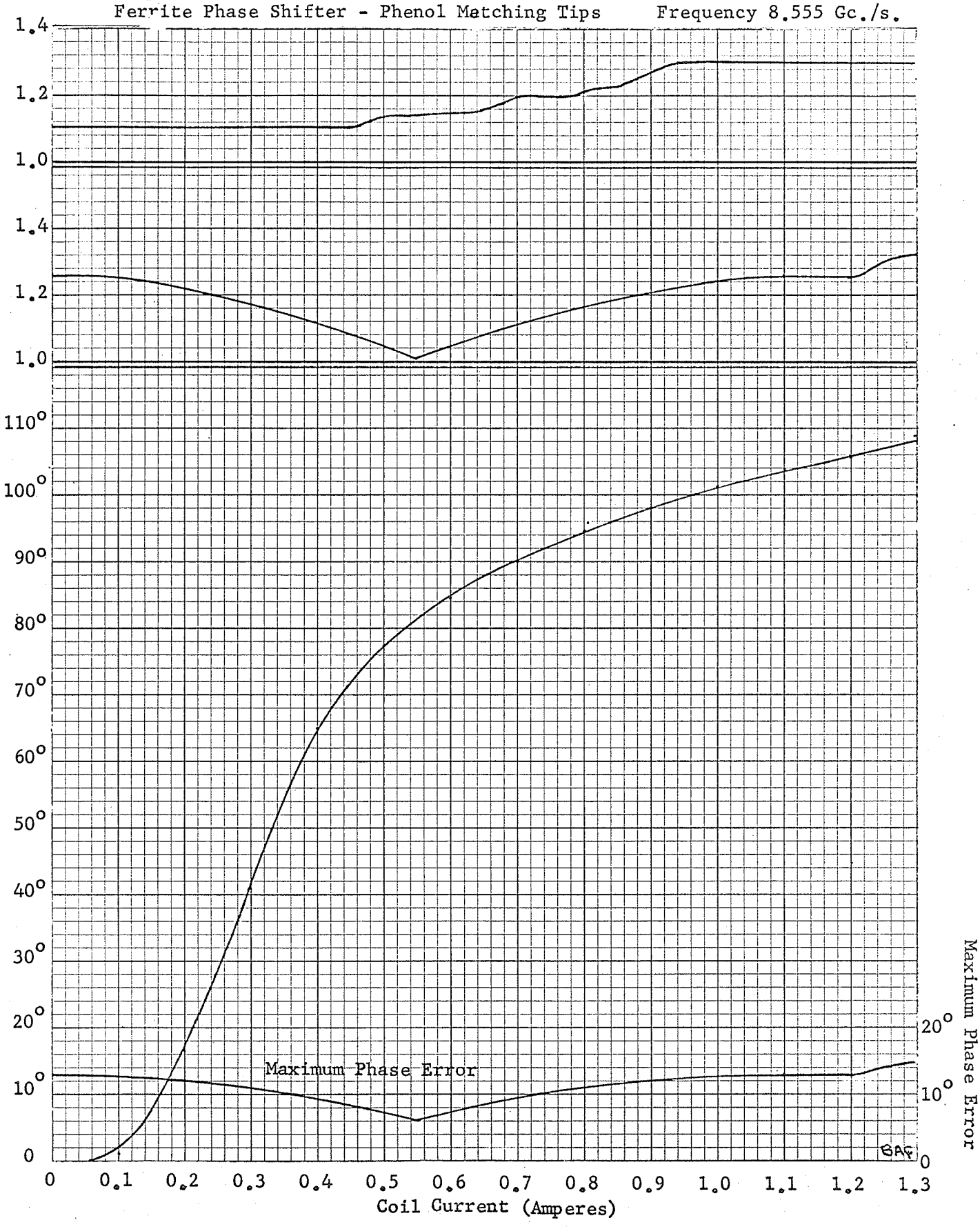

Graph 3.3
Ferrite Phase Shifter - Phenol Matching Tips Frequency 9.014 Gc./s.

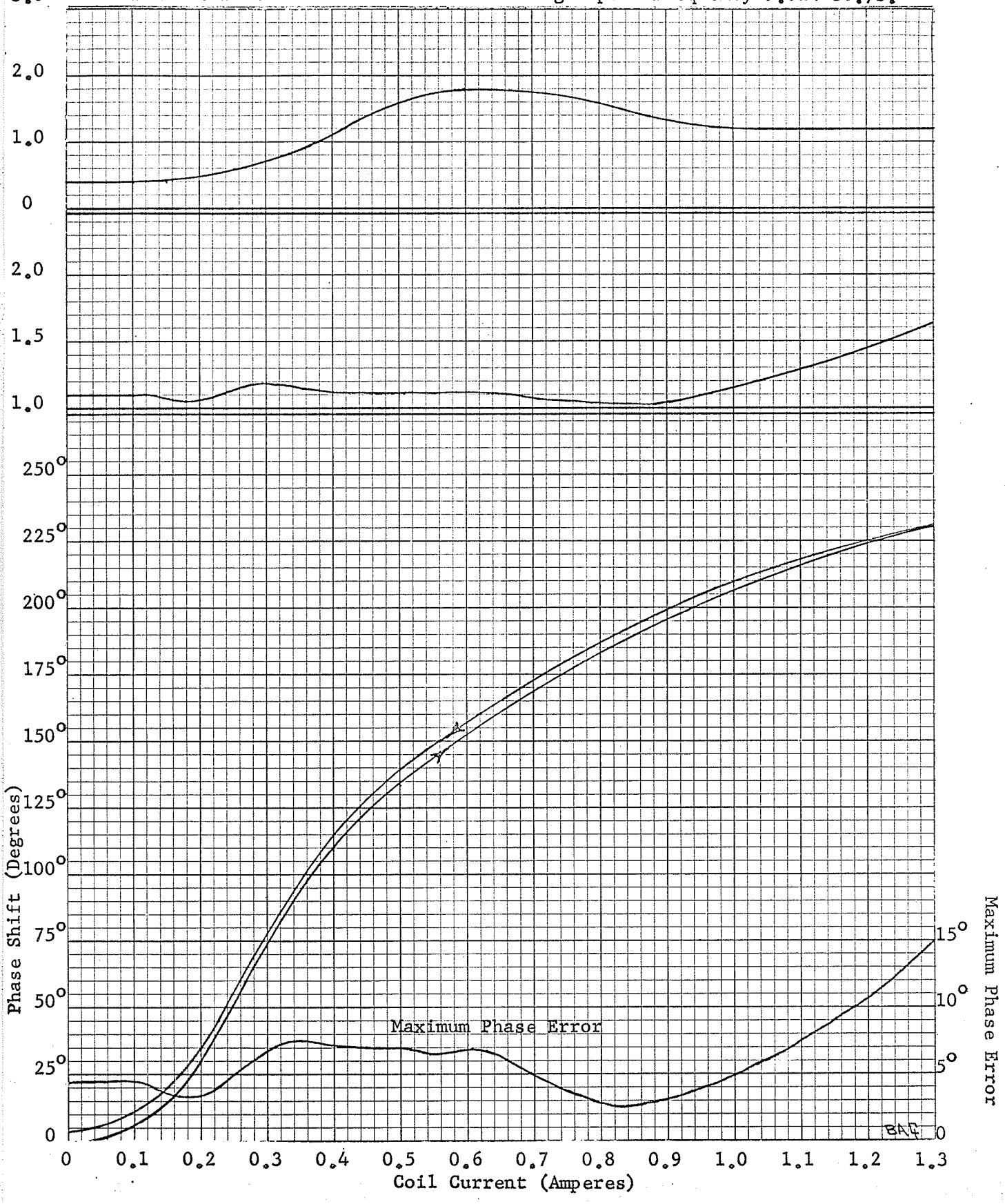

Graph 3.4
Ferrite Phase Shifter - Phenol Matching Tips Frequency 9.390 Gc./s.

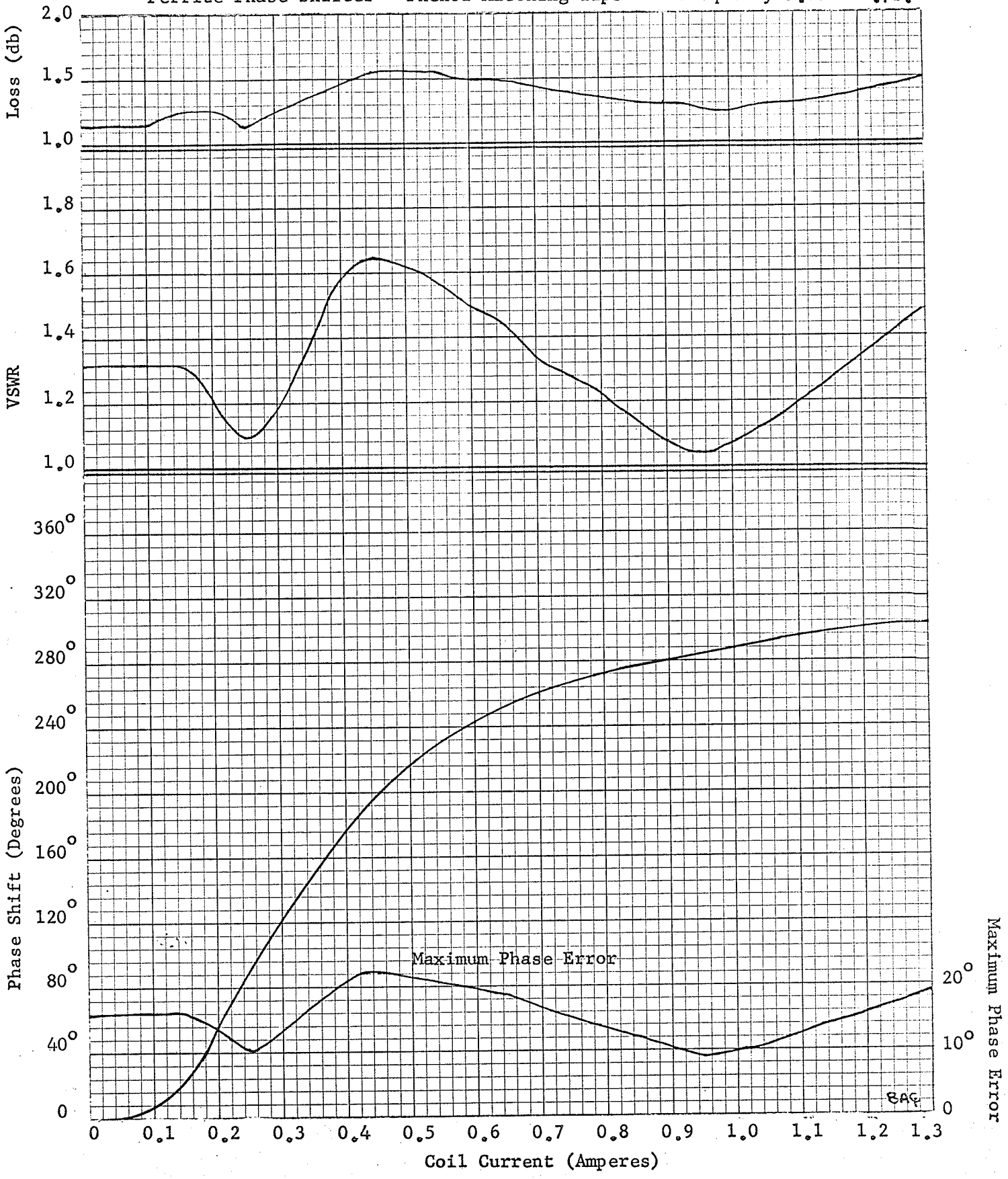

Graph 3.5
Ferrite Phase Shifter - Phenol Matching Tips Frequency 9.747 Gc./s.

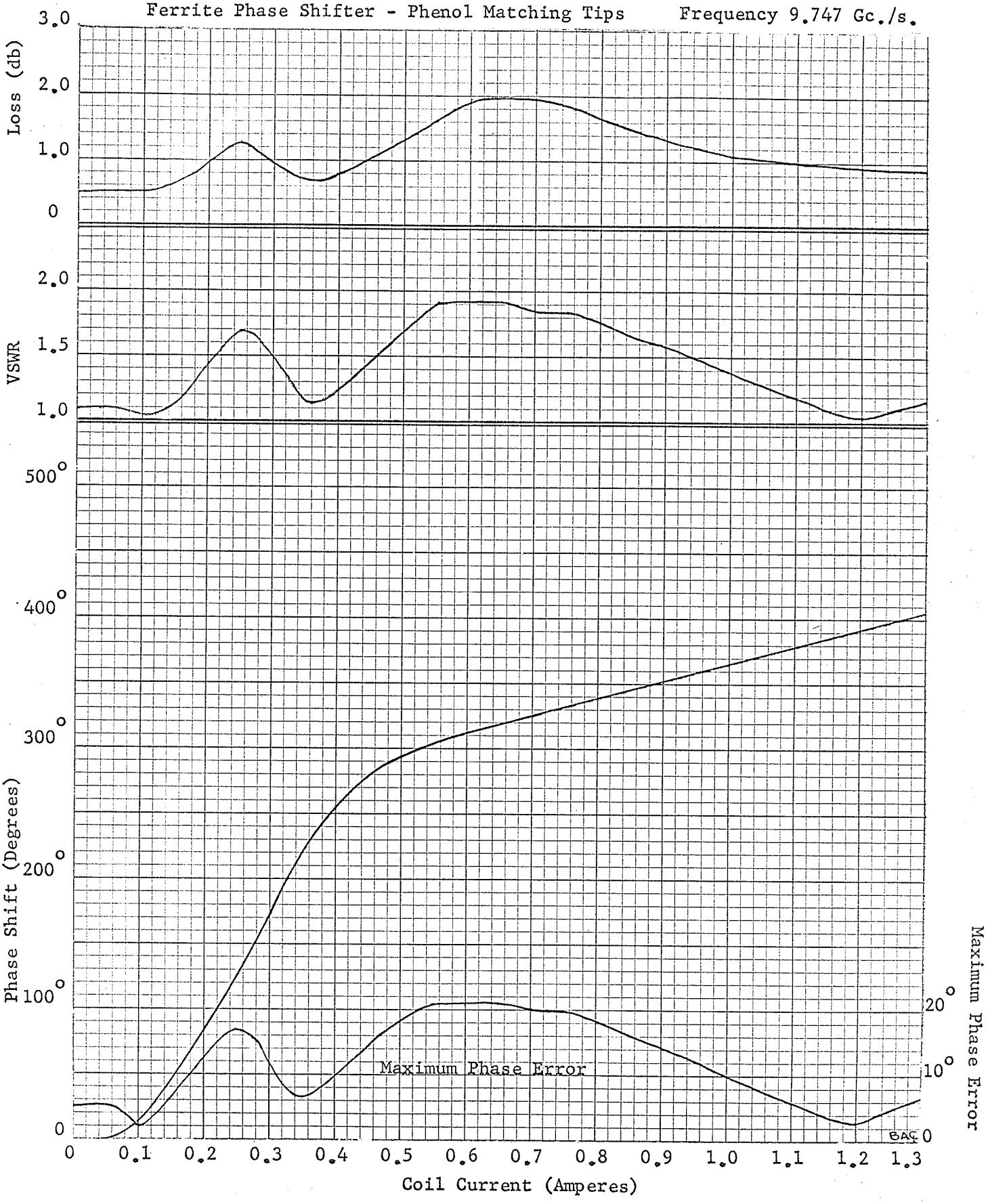

Graph 3.6
Ferrite Phase Shifter - Phenol Matching Tips Frequency 10.106 Gc./s.

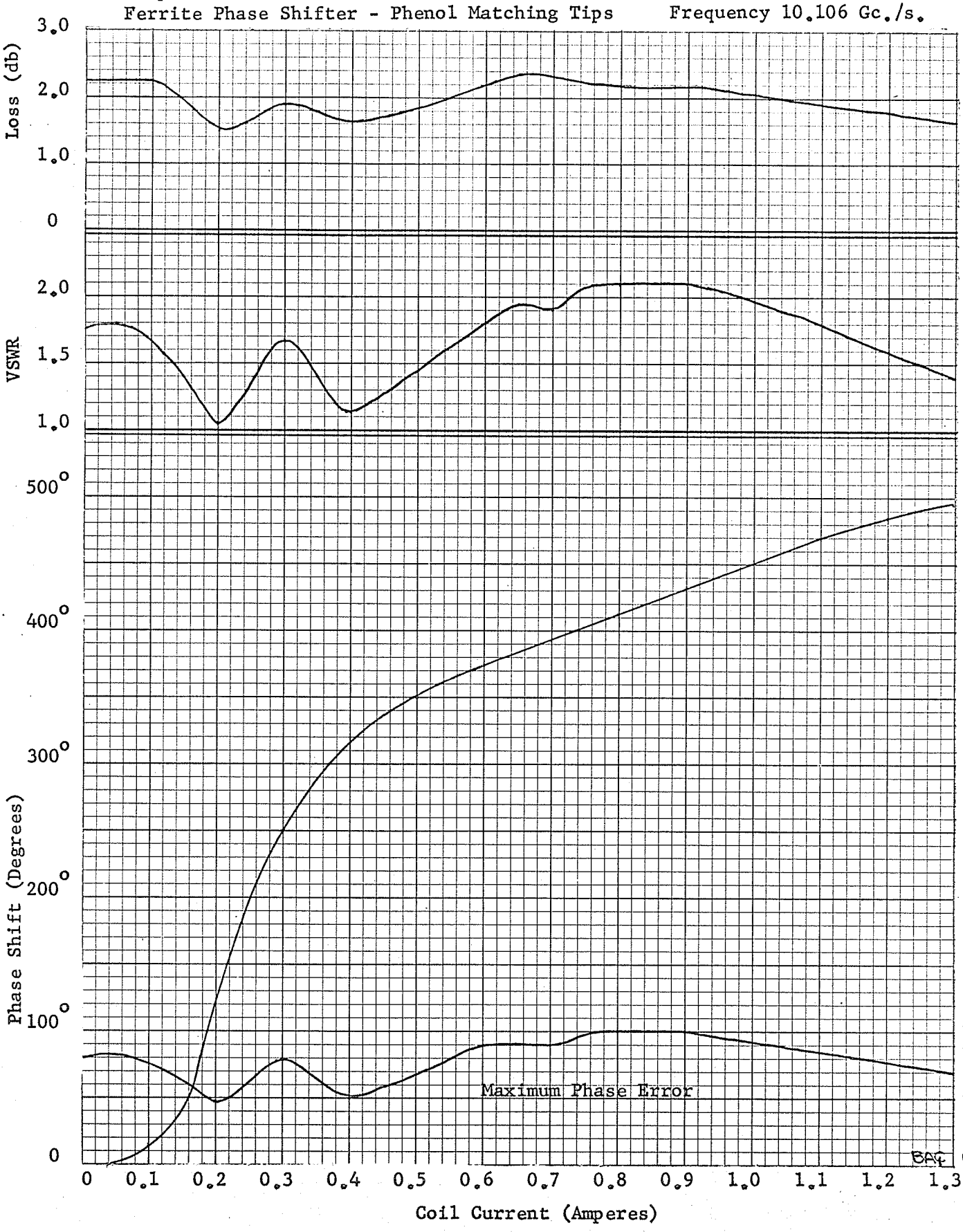

Graph 3.7
Saturation Phase Shift at Test Frequencies - Phenol Matching Tips

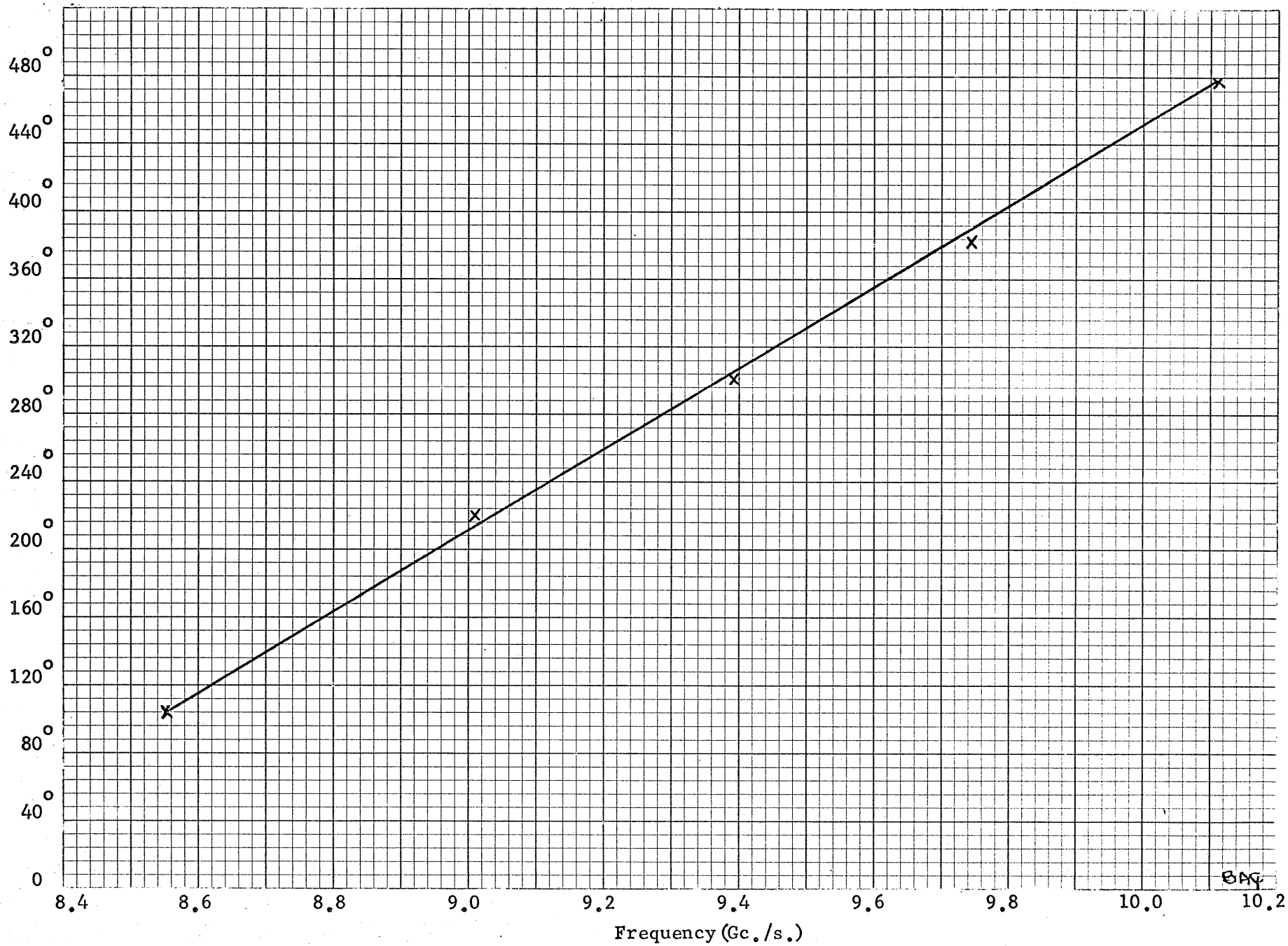

Graph 3.8
Variation in Insertion Loss with Field at 11.120 Gc./s. - Phenol Matching Tips

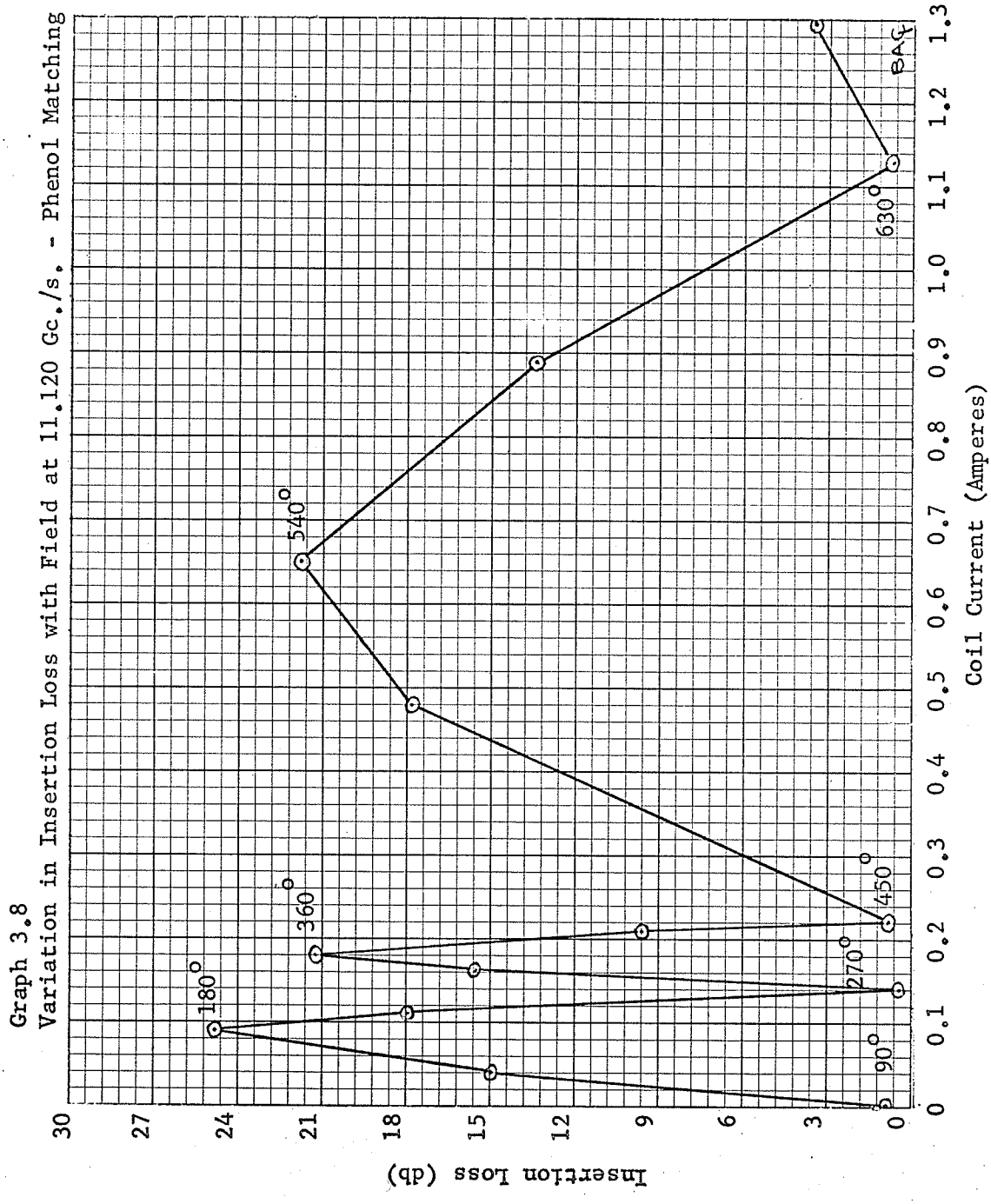

Graph 3.9
Phase Shifter Characteristics - Ferrite Matching Tips

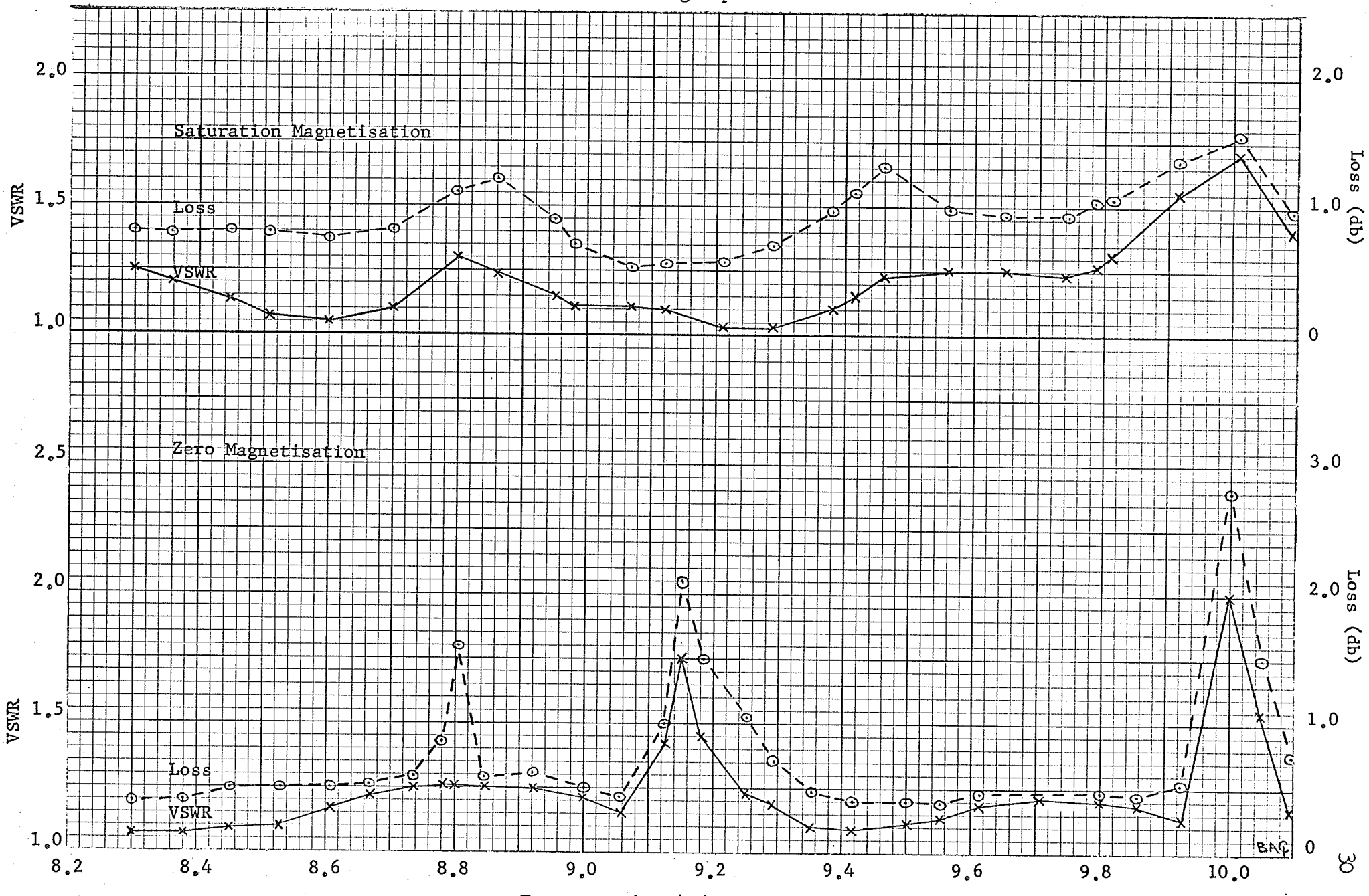

Graph 3.10
Ferrite Phase Shifter - Ferrite Matching Tips Frequency 8.558 Gc./s.

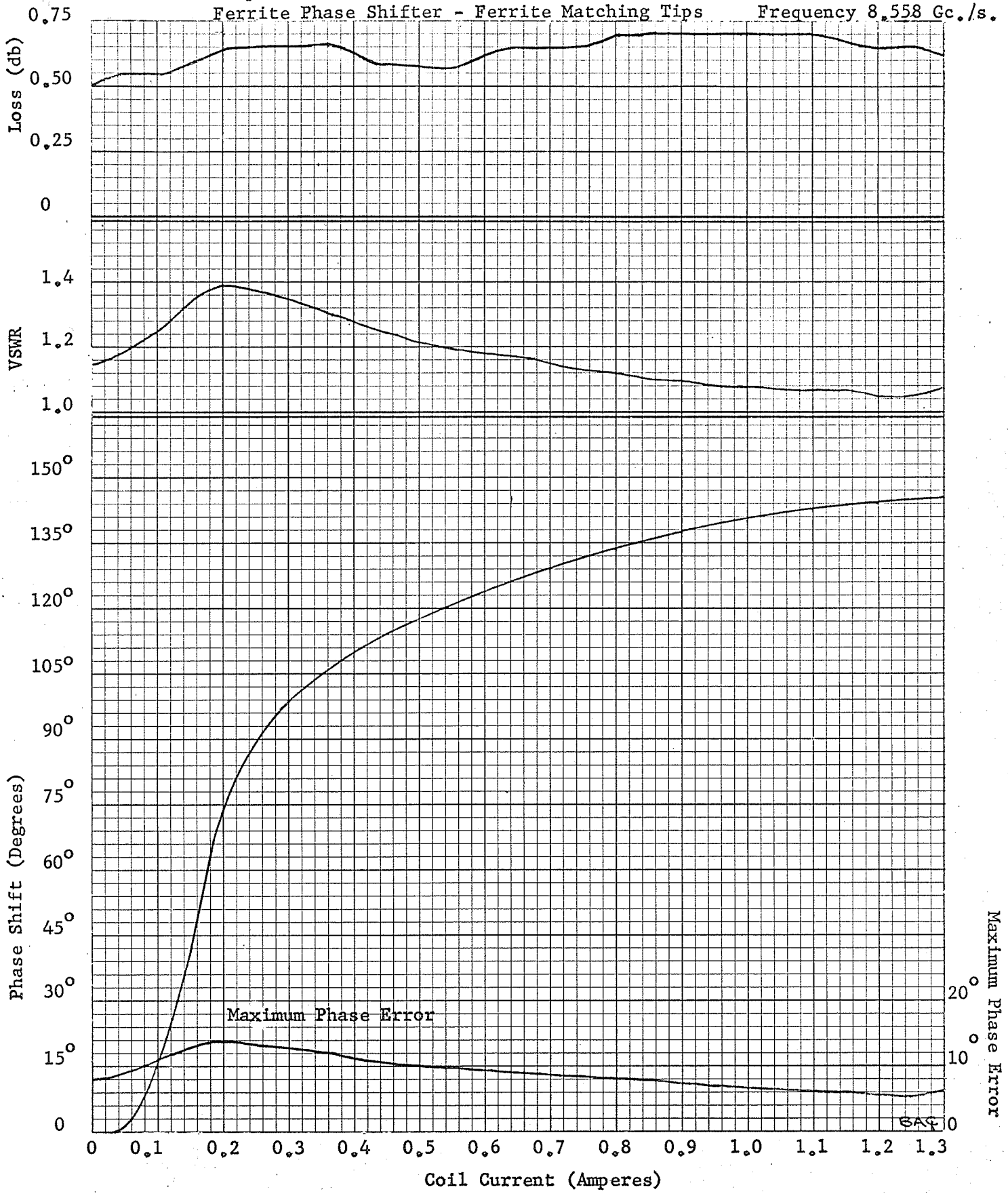

Graph 3.11
Ferrite Phase Shifter - Ferrite Matching Tips Frequency 9.005 Gc./s.

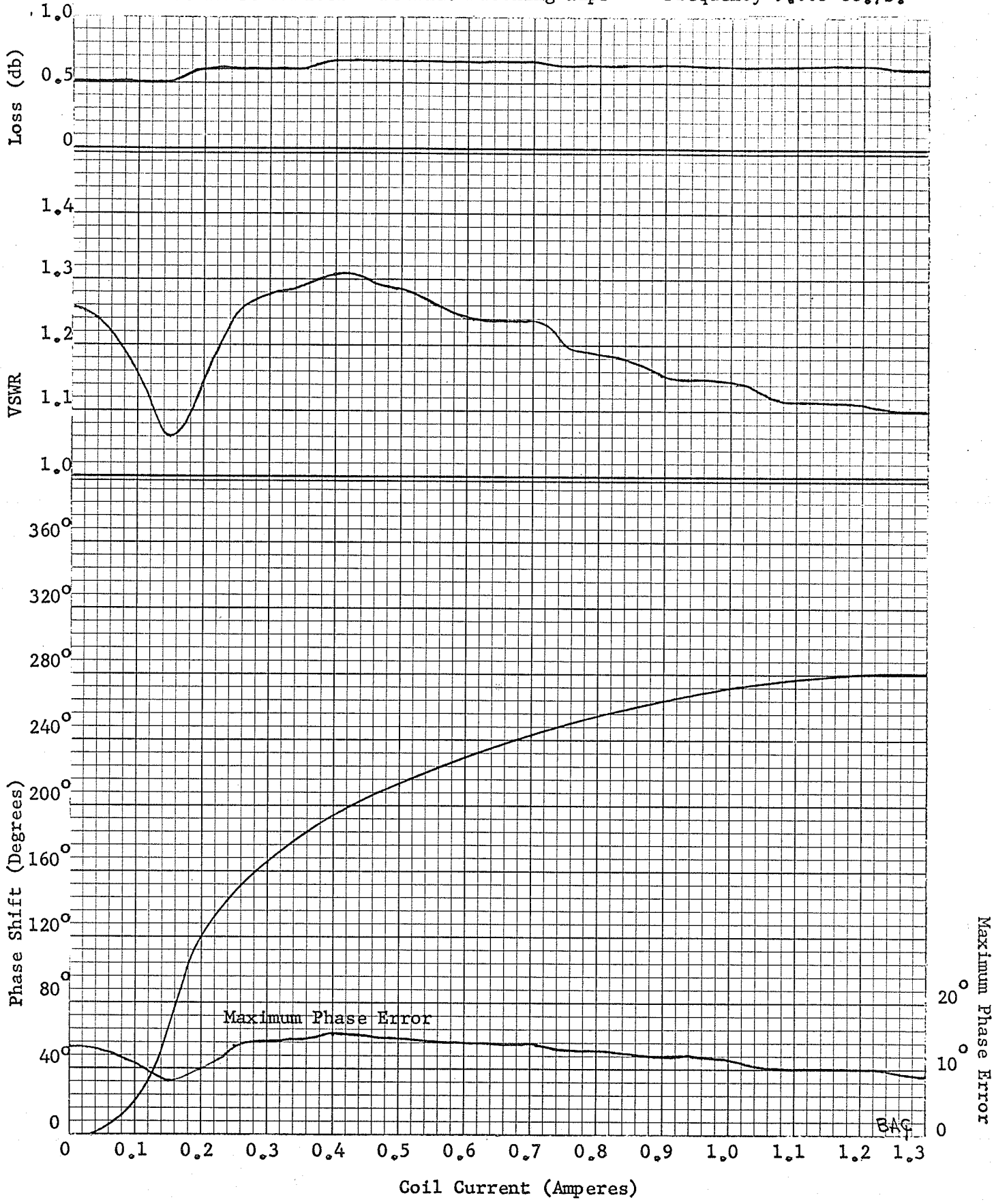

Graph 3.12

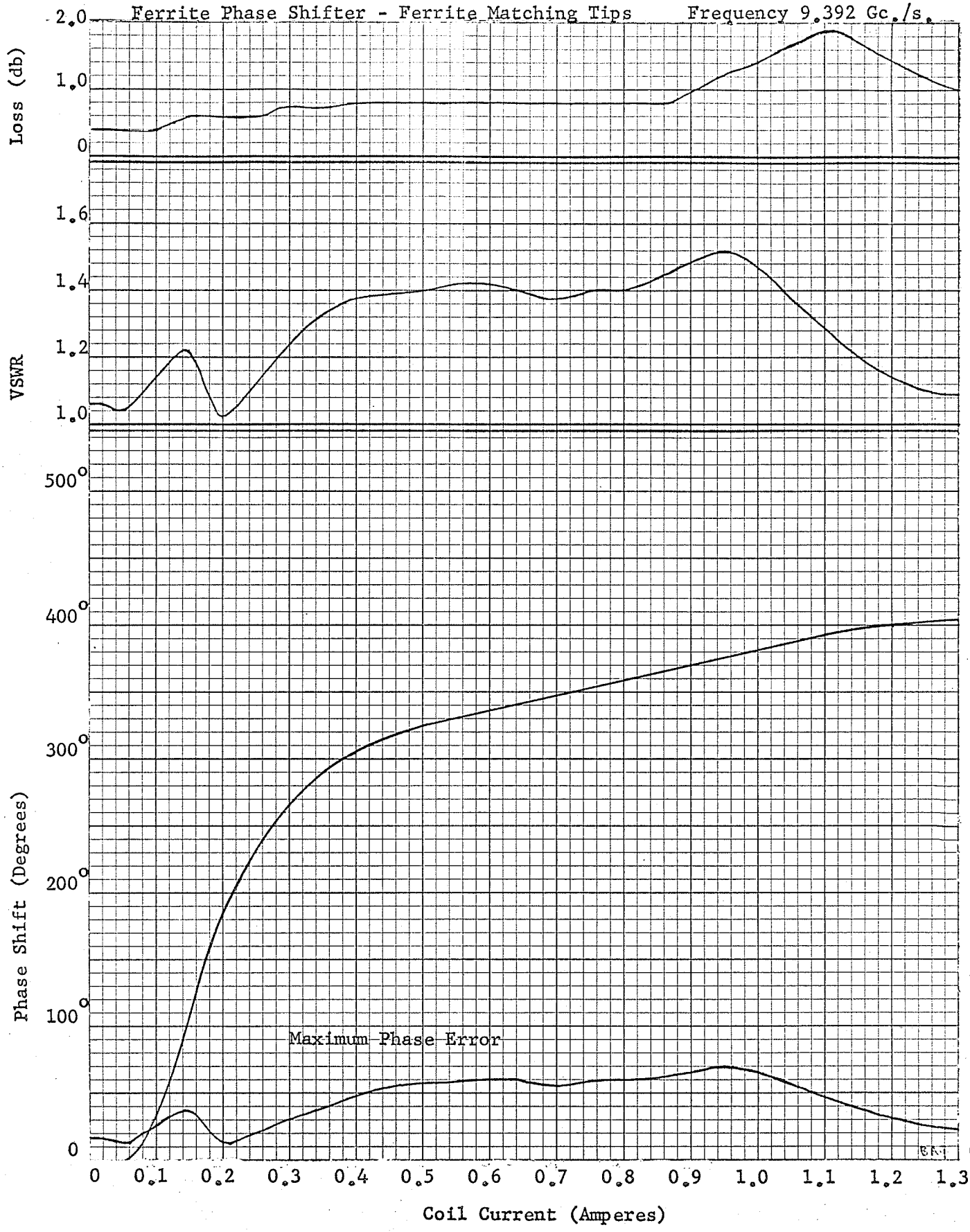
Ferrite Phase Shifter - Ferrite Matching Tips
Frequency 9.392 Gc./s.
Loss (db)
2.0
1.0
0
VSWR
1.6
1.4
1.2
1.0
Phase Shift (Degrees)
500°
400°
300°
200°
100°
0
Maximum Phase Error
20°
10°
0
Maximum Phase Error
0
0.1
0.2
0.3
0.4
0.5
0.6
0.7
0.8
0.9
1.0
1.1
1.2
1.3
Coil Current (Amperes)

Graph 3.13
Ferrite Phase Shifter - Ferrite Matching Tips Frequency 9.748 Gc./s.

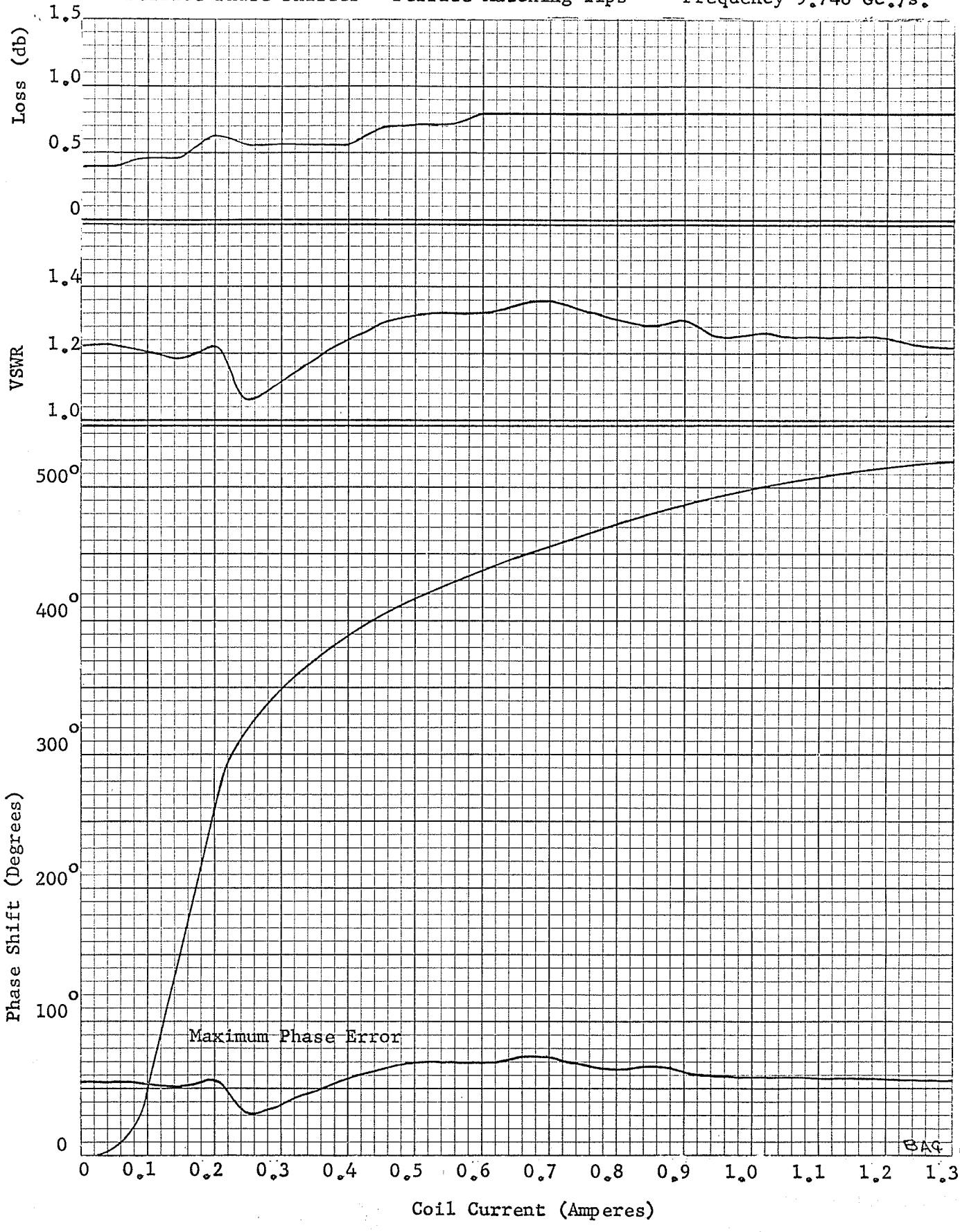

Graph 3.14
Ferrite Phase Shifter - Ferrite Matching Tips Frequency 10.107 Gc./s.

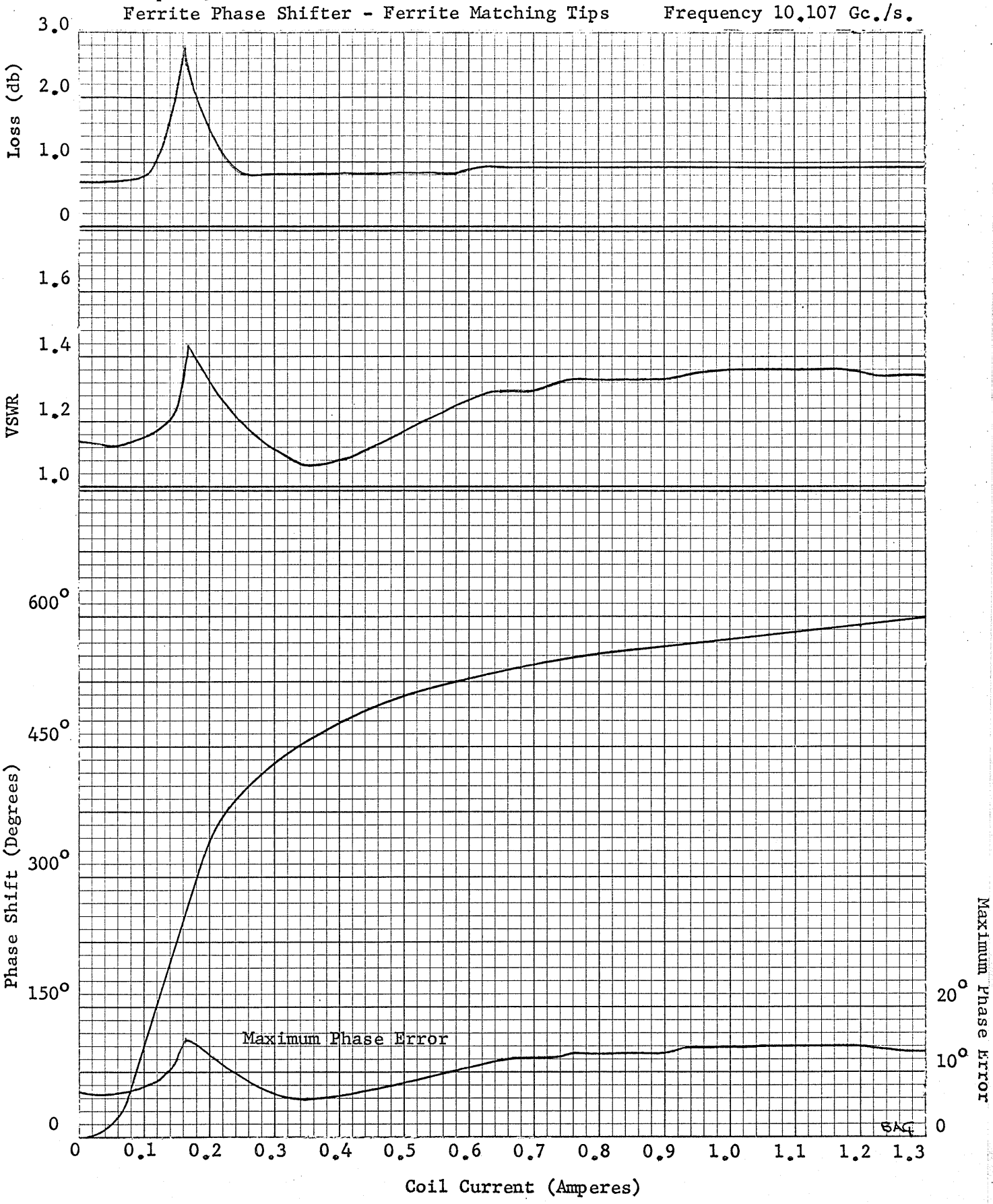

Graph 3.15
Saturation Phase Shift at Test Frequencies - Ferrite Matching Tips

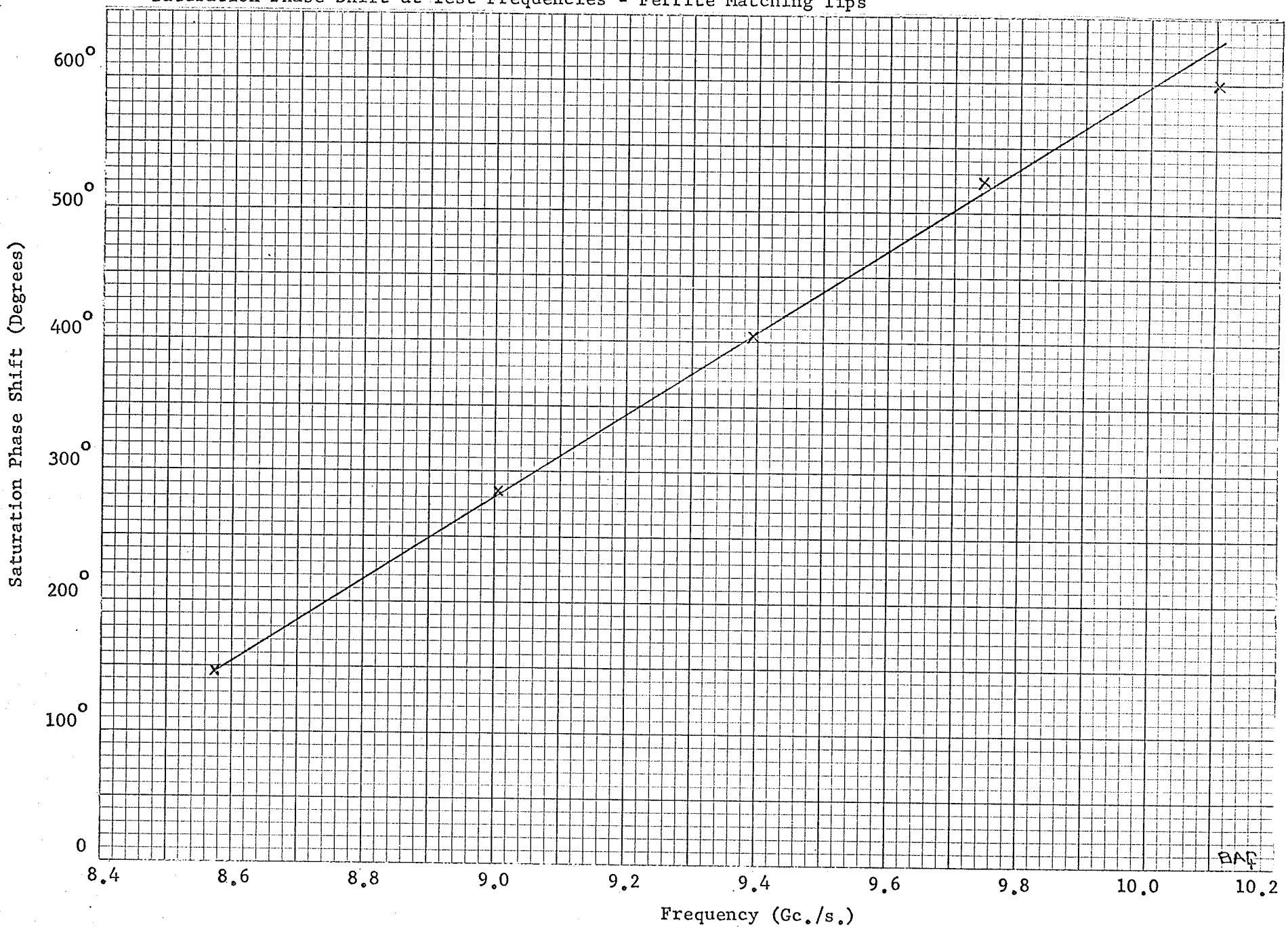

Graph 3.16
Normalized Saturation Phase Shift for Both Matching Systems

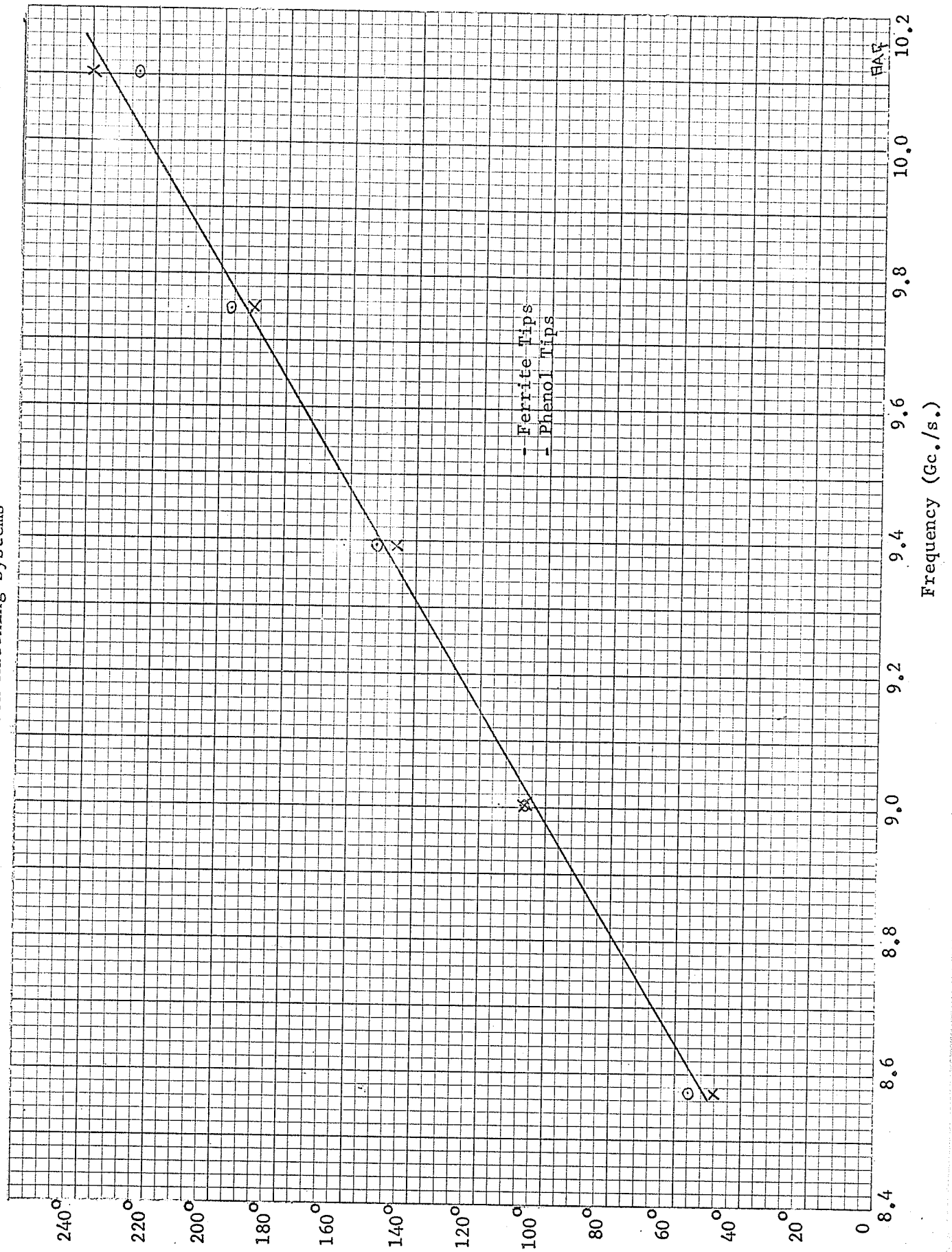

CHAPTER IV

THEORETICAL CONSIDERATIONS

Unfortunately, no rigorous mathematical theory applicable to the phase shifting assembly of this thesis exists, and no attempt will be made to present one here. The best qualitative explanation of the device is contained in a theoretical argument propounded by Weiss.[16] This theory is based upon observed phenomena. For a complete description of this phenomenological theory, the reader is referred to the original article.[16] Only the major points will be outlined in this study.

4.1 The Weiss Phenomenological Theory

According to this theory, single mode propagation occurs for a saturated ferrite for a range of frequencies determined by the ferrite rod diameter. This propagating mode is elliptically polarised. Above a certain critical frequency, a second mode, also elliptically polarised breaks into propagation. (By referring to graph 3.1, it can be seen that large fluctuations in VSWR and loss occur above 10.0 Gc./s. These fluctuations signal the onset of one or more higher order modes.)

The combination of these two elliptically polarised modes is a linearly polarised wave. Since the velocities of propagation are different for the two propagating modes,

the plane of linear polarisation of the resultant wave will rotate as the wave propagates along the structure. The direction of linear polarisation that it has at the output end of the ferrite section determines whether it will be coupled to the succeeding empty waveguide or whether it will be wholly or partially reflected. Since the empty rectangular waveguide following the ferrite section can accept radiation that is vertically polarised only (TE_{10} mode), the horizontal component will be totally reflected.

As the frequency is increased above the critical value, the plane of linear polarisation at the output of the ferrite structure will rotate. At certain unique frequencies, the plane of polarisation will be vertical, coupling to the empty waveguide will be a maximum, and loss will be a minimum. At frequencies approximately halfway between the above frequencies, the plane of polarisation will be horizontal and almost total reflection will occur. Therefore, the insertion loss will be a maximum. Reference to graph 3.1 will clarify this phenomenon.

Fluctuations in transmission loss at a single frequency (above the critical frequency) also occur as the ferrite is subjected to successively stronger direct magnetic fields. The phase velocities of both propagating modes will be the same at zero magnetisation level

since the ferrite is isotropic. As the magnetisation is increased, the phase velocity for one mode increases, and the phase velocity for the other decreases. Thus a rotation of the resultant plane of linear polarisation occurs and the insertion loss passes through alternate minima and maxima as the plane of polarisation alternates between vertical and horizontal. This combination of the two propagating modes explains the Faraday rotation-loss encountered in the previous chapter and illustrated in graph 3-8.

As to the origin of the phase shift, Weiss contends that it is produced primarily by the change with magnetisation of the diagonal component (μ) of the permeability tensor. (This variation of μ with applied field is illustrated for Ferramic R-1 in figure 1, appendix I.) It appears that the off-diagonal component (α) plays a secondary role in the production of phase shift.

Working on this premise, Weiss attempted to extract quantitative phase shift information by comparison of the ferrite phase shifter with the case of an isotropic dielectric rod mounted axially in a circular waveguide. The agreement between phase shift values so predicted, and those experimentally observed was only fair. This author believes that much closer agreement could be achieved through comparison of the ferrite rod assembly with the case of an unbounded dielectric rod waveguide.

4.2 Comparison of Ferrite Rod Structure to a Dielectric Rod Waveguide

The justification for an attempt to correlate the behaviour of a ferrite rod-loaded rectangular waveguide with a dieletric rod waveguide is the fact that the relative dielectric constant of the ferrite is large (ϵ =13.6). This fact means that the preponderance of microwave energy is contained within the ferrite and, therefore, the metal walls of the waveguide have lost their central role in confining the energy. Therefore they could be removed without appreciably affecting field configurations and energy distributions. Following this reasoning, the conclusion may be drawn that change in the propagation properties of the ferrite loaded waveguide are solely due to changes in the properties of the ferrite itself.

The solution of the trancendental eigenvalue equation of a dielectric rod waveguide must be done graphically or by a trial and error method. The dominant mode is the hybrid dipole mode which has no lower cutoff frequency.[17]

The eigenvalue equation for the dominant hybrid dipole mode (following Collin[18]) is:

$$\left[\frac{\epsilon_1 J_1'(ha)}{h J_1(ha)} - \frac{K_1'(pa)}{p K_1(pa)}\right]\cdot\left[\frac{J_1'(ha)}{h J_1(ha)} + \frac{K_1'(pa)}{p K_1(pa)}\right]$$

$$= \left[\frac{\beta_g}{k_0}\,\frac{(p^2+h^2)}{p^2 h^2}\right]^2$$

Where ϵ_1 - permittivity of the dielectric rod material

$h = \sqrt{\epsilon_1 k_o^2 - \beta_g^2}$

$p = \sqrt{\beta_g^2 - k_o^2}$

β_g - waveguide propagation constant

$k_o^2 = \omega^2 \mu_o \epsilon_o$

a - rod radius = .125"

$J_1(ha)$ - Bessel function of the 1st kind, 1st order

$J_1'(ha)$ - 1st derivative of $J_1(ha)$

$K_1(pa)$ - Modified Bessel of the 2nd kind, 1st order

$K_1'(pa)$ - 1st derivative of $K_1(pa)$

The eigenvalue equation was solved through use of a trial and error method that was programmed on the I. B. M. 1620 computer.

In order to compare the phase shift predicted by solutions to the above equation, to observed phase shift, the following identification was made. The $\mu\epsilon$ product for the ferrite was assumed equivalent to the permittivity (ϵ_1) of the dielectric of the rod waveguide. This equivalence is strictly true for the case of plane waves only, but this identification is not inconsistent with the approximate nature of the entire comparison method.

At zero magnetisation level the diagonal component of the permeability tensor is 0.76 and the permittivity 13.6 (see appendix I). The $\mu\epsilon$ product is therefore 10.3. When the ferrite is saturated, the diagonal component

increases to 1.0 and the $\mu\epsilon$ product to 13.6. Therefore the eigenvalue equation was solved for the propagation constant (β_{g_1}) with $\mu\epsilon$ = 10.3 and then it was solved for the propagation constant (β_{g_2}) with $\epsilon_1 \equiv \mu\epsilon$ = 13.6. Now β_{g_1} represents the phase shift / unit length in the unmagnetised rod and β_{g_2} represents the specific phase shift in the saturated case. Therefore the change in phase shift (or simply phase shift as defined in chapter II) is equal to ($\beta_{g_2} - \beta_{g_1}$) times the length of the ferrite rod (2 inches). The phase shift so calculated is the predicted saturation phase shift and it was calculated for assorted X-band frequencies. The excellent agreement between predicted and measured saturation phase shifts, for the phenol tipped configuration, is apparent from graph 4.1. The predicted values are 30° or less lower than the observed values at all frequencies.

It is interesting to note that although the hybrid dipole mode has no lower cutoff frequency (or no minimum rod diameter) there exists a minimum frequency (or rod diameter) below which the rod loses its central role in the guiding of the radiation. Comparison of the single frequency data of Reggia[a] and the predicted change in phase

---

[a] The experimental data displayed on graph 4.2 was obtained from figure 4 of reference #15.

shift with rod diameter, emphasizes this point. Referring to figure 4.2, it is seen that below a critical rod diameter both the experimental saturation phase shift (Reggia) and the saturation phase shift predicted by dielectric rod waveguide theory become very small. Hence, the preponderance of the energy must exist outside the rod since changes in permeability due to magnetisation affect propagation only slightly.

Another important feature of the comparison of the ferrite structure to the unbounded dielectric rod, is the ability of the dielectric rod theory to predict the onset of higher order modes. The next higher order mode on the dielectric rod is the TM_{01} mode.[19] The cut-off frequency for this mode is given by:

$$f_c = \frac{2.405\,c}{2\pi a\sqrt{\epsilon_1 - 1}} \quad \text{cps}$$

Where c - velocity of light in free space
a - rod radius = .125"
ϵ_1 - permittivity of dielectric material

If the identification of the $\mu\epsilon$ product of the ferrite with the permittivity (ϵ_1) of the dielectric is continued, the cutoff frequency of the TM_{01} in the saturated ferrite can be calculated. At saturation, $\mu\epsilon = 13.6$. The mode will then propagate above a frequency of approximately 10.0 Gc./s. This value agrees with the experimentally

determined frequency above which higher order modes are propagating in the saturated ferrite. (See figure 3.1).

Graph 4.1
Comparison of Predicted & Measured Saturation Phase Shifts - Phenol Matching Tips

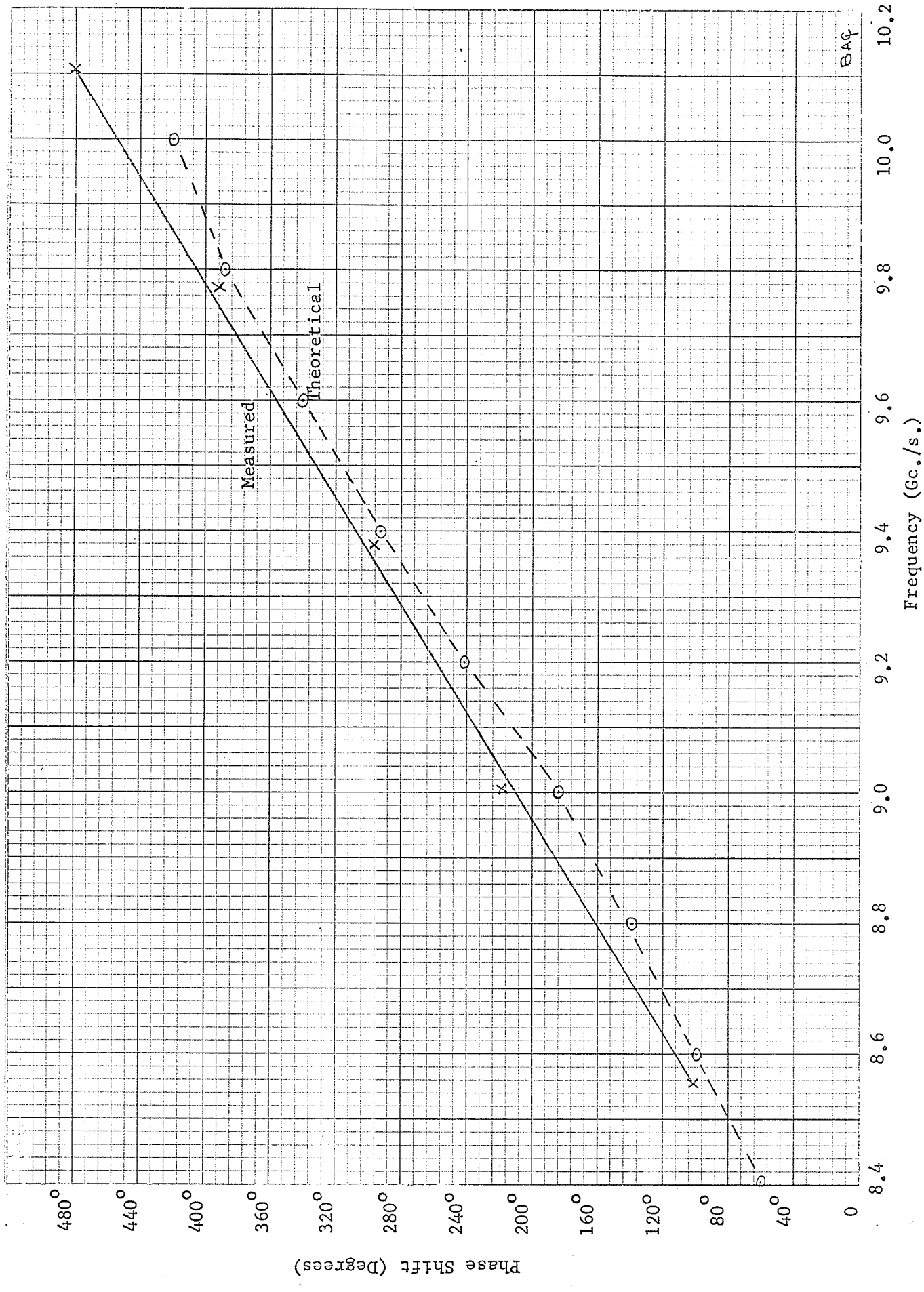

Graph 4.2
Comparison of Measured & Predicted Saturation Phase Shifts - Frequency 9.100 Gc./s.

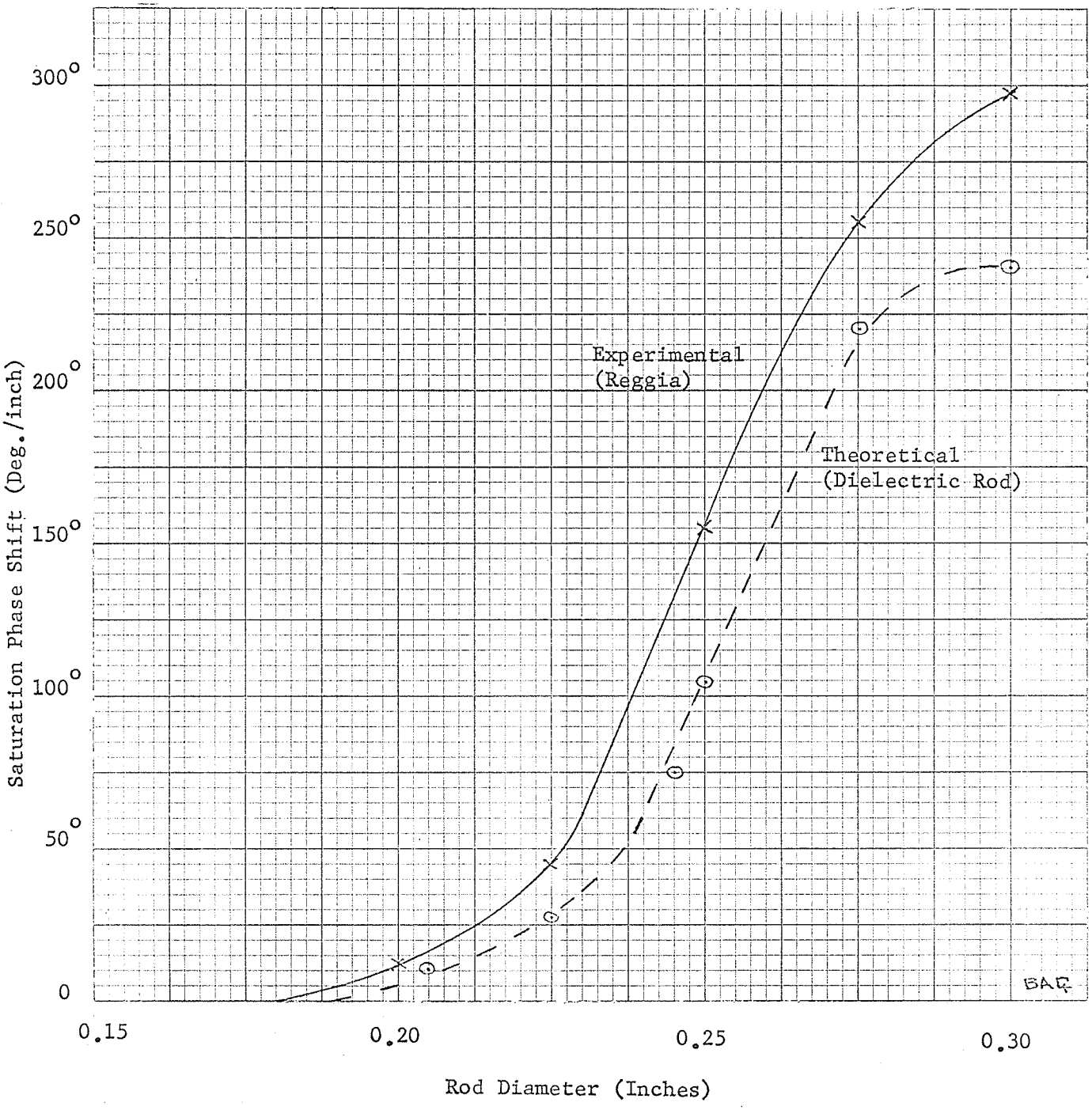

CHAPTER V

CONCLUSIONS AND FUTURE STUDY

5.1 Conclusions

The phase shifting device described in this thesis provides a relatively simple way of varying the phase of a microwave signal. Large reciprocal phase shifts are available with small variations in control current. Although phase delays only are attainable with this configuration, appropriate biasing would allow the phase to be advanced or retarded with respect to the bias phase. The device is extremely frequency sensitive--the phase shift at any magnetisation level being approximately proportional to the frequency. The usable frequency range of this phase shifter extends from the lower limit of X-band to about 10.0 gc., where the onset of higher order modes produce wide fluctuations in transmitted power.

It was found that matching over the productive frequency range of the phase shifter was quite difficult. Ferrite matching tips were found to give a slight improvement over phenol matching tips in VSWR at the test frequencies, but overall, the amendment was not significant. Matching at a single frequency could be accomplished by means of a slide screw tuner or E-H tuner, but this match would only hold over a certain range of magnetisation levels.

(Reference to graph 3.4, for instance, illustrates that the VSWR is a function of the magnetisation level at a single frequency.) Transmission loss through the device was found to be due primarily to reflection and consequently more effective matching would lower the loss.

Hysteresis was found to affect the phase shift at any current setting but its effect could not be accurately determined, since errors inherent in the phase measuring technique were usually large enough to render extraction of numerical hysteresis data impossible.

The device should show a certain amount of thermal sensitivity, since all the properties of the ferrite are temperature sensitive. No attempt was made to determine quantitative thermal effects, but it is felt that the failure of the ferrite to saturate completely at high magnetisation levels was due to coil heating. Confirmation of the fact that the phase shift at any current setting increases with temperature is found in the literature.[23]

5.2 Future Study

Other than the obvious applications of this device, as a phase shifter, there are some other possible uses that bear investigation. There arises the possibility of a phase or frequency modulation system or even an amplitude modulator that would utilize the phase sensitive properties of a magic tee.

Development of improved wideband matching schemes deserves some study, but the problem is a particularly thorny one and possibly the best compromise would be better matching over a reduced bandwidth.

An interesting problem in non-linear control system theory would be the reduction of the phase shifter to a frequency insensitive device. This would involve a frequency sensitive component that controlled the bias current to produce a constant phase shift over a certain frequency band.

Investigation of hysteresis effects and thermal drifts and methods to counteract these undesirable properties of ferrite, would also find practical interpretations. Devices for the neutralization of hysteresis and thermal drifts have been studied.[20]

Location of the ferrite rod centrally in the rectangular waveguide produces reciprocal phase shift, but off-setting the rod to either side of the guide would result in non-reciprocal phase shifts, i.e. the phase shift would depend on the direction of propagation. Use of non-reciprocal phase shifters in circulators and duplexers render investigation of a device of this sort inevitable. A different phase measuring technique than the one described in this study would have to be developed, however, since this technique applies to reciprocal devices only.

BIBLIOGRAPHY

1. Kales, M.L., Modes in Waveguides Containing Ferrites. Journal of Applied Physics, 1953. Vol. XXIV, pp. 604 - 608.

2. Suhl, H., and Walker, L.R., Topics in Guided Wave Propagation Through Gyromagnetic Media. Bell System Technical Journal, 1954. Vol. XXXIII, pp. 579 - 659, 939 - 986, 1133 - 1194.

3. Waldron, R.A., Theory of Mode Spectra of Cylindrical Waveguides Containing Gyromagnetic Media. Journal of the British Institution of Radio Engineers, 1959. Vol. XIX, pp. 347 - 356.

4. Sakiotis, N.G., and Chait, H.N., Ferrites at Microwaves. Proc. IRE, 1953. Vol. XLI, pp. 87 - 93.

5. Ljung, P.E., Development of a Rotation Isolator for 6 cm. Wavelength. Proc. IEE, 1957. Vol. CIVB, Supplement 6, pp. 362 - 363.

6. LeCraw, R.C., High-speed Magnetic Pulsing of Ferrites. Journal of Applied Physics, 1954. Vol. XXV, p. 678.

7. Ohm, E.A., A Broadband Microwave Circulator. IRE. Transactions of Microwave Theory and Technique, 1956. Vol. IV, p. 210.

8. Fox, et al, Behaviour and Applications of Ferrites in the Microwave Region. Bell System Technical Journal, 1955. Vol. XXXIV, pp. 5 - 103.

9. Button, K.J., Theoretical Analysis of the Field-Displacement Isolator. IRE. Transactions on Microwave Theory and Technique, 1958. Vol. VI, pp. 303 - 308.

10. Kales, et al, A Nonreciprocal Microwave Component. Journal of Applied Physics, 1953. Vol. XXIV, p. 816.

11. Chait, H.N., and Curry, T.R., Y-Circulator. Journal of Applied Physics, 1959. Vol. XXX, p. 1525.

12. Waldron, R.A., Ferrites - An Introduction for Micro-Wave Engineers. London: D. Van Nostrand, 1961. Chap. 3.

13. Polder, D., On the Theory of Ferromagnetic Resonance. Philosophical Magazine, 1949. Vol. XL, pp. 99 - 115.

14. Magid, M., Precision Microwave Phase Shift Measurements. IRE. Transactions on Instrumentation, 1958. Vol. VII, p. 321.

15. Reggia, F., and Spencer, E.G., A New Technique in Ferrite Phase Shifting for Beam Scanning of Microwave Antennas. Proceedings of the IRE, 1957. Vol. XLV, pp. 1510 - 1517.

16. Weiss, J.A., A Phenomenological Theory of the Reggia-Spencer Phase Shifter. Proc. IRE, 1959. Vol. XLVII, pp. 1130 - 1137.

17. Schelkunoff, S.A., Electromagnetic Waves. Princeton, New Jersey: D. Van Nostrand, 1943. Pp. 425 - 428.

18. Collin, R.E., Field Theory of Guided Waves. New York: McGraw-Hill, 1960. P. 482.

19. Ramo, S., and Whinnery, J.R., Fields and Waves in Modern Radio. New York: John Wiley and Sons, Inc., 1960. P.390.

20. King et al, Precise Control of Ferrite Phase Shifters. IRE. Transactions on Microwave Theory and Technique, 1959. Vol. VII, p. 229.

21. Reggia, F., A New Broadband Absorption Modulator. IRE. Transactions on Microwave Theory and Technique, 1961. Vol. IX, p. 343.

22. Schafer, G.E., Mismatch Errors in Microwave Phase Shift Measurements. IRE. Transactions of Microwave Theory and Technique, 1960. Vol. VIII, p. 617.

23. Lax, B., and Button, K.J., Microwave Ferrites and Ferrimagnetics. New York: McGraw-Hill Book Co., Inc., 1962. Sec. 12 - 8, p. 608, Figure 12-48a.

24. Kajfez, D., Wide-band Matching of Lossless Waveguide Two-Ports. IRE. Transactions on Microwave Theory and Technique, 1962. Vol. X, pp. 154 - 158.

APPENDIX I

MICROWAVE PROPERTIES OF FERRAMIC R-1

Ferramic is a lowloss MnMg ferrite manufactured by General Ceramic Corporation. The electromagnetic properties of Ferramic R-1 at X-band are summarized below:[21]

Permittivity - 13.6
Saturation magnetisation @ 25°C - 1760 gauss

For the variation of μ and α with applied field at 9.340 Gc., see graph AI.1.

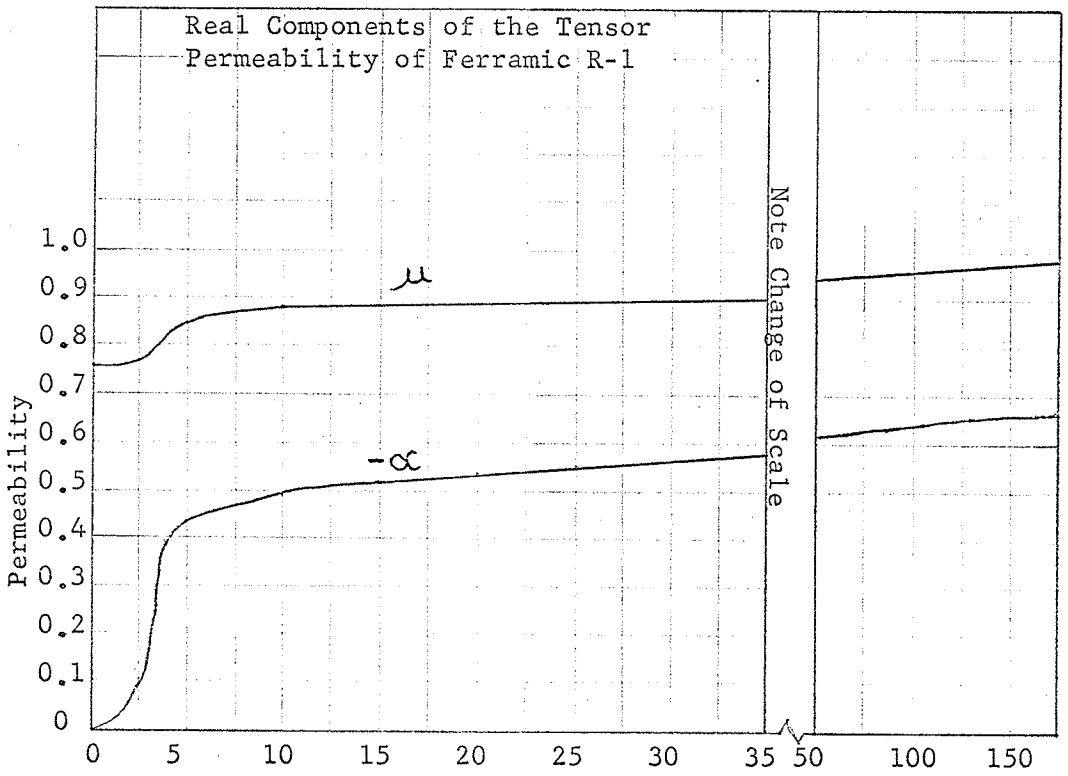

Graph AI.1

APPENDIX II

DERIVATION OF PHASE ERROR

The following derivation of the error associated with the phase measuring technique, is due primarily to Schafer.[22] Derivations from Schafer occur where it is felt that the approximations used are not justifiable.

Consider a test component in the phase measuring configuration, terminated with a short circuit. (Figure AII.1)

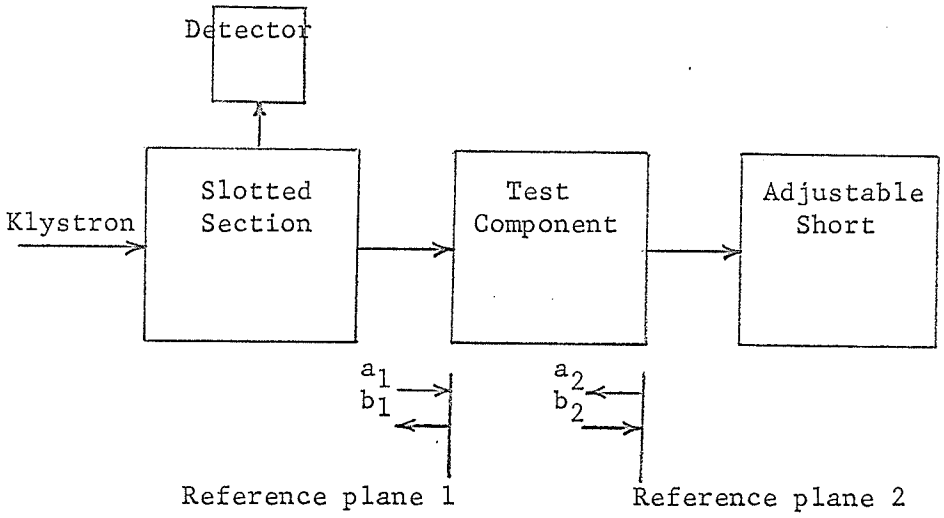

Figure AII.1

where a_1 - amplitude of wave incident upon input of test component. (At reference plane 1)

b_1 - amplitude of wave reflected from input.

a_2 - amplitude of wave incident upon output of test component. (At reference plane 2)

b_2 - amplitude of wave incident upon short. (At reference plane 2)

Observe that if the short is perfectly reflecting, $|a_2| = |b_2|$.

Now the input reflection coefficient, $\rho_1 = b_1/a_1$.

A minimum occurs in the standing wave pattern when:

$$\text{Arg } \rho_1 = \text{Arg } b_1/a_1 = (2n+1)\pi$$

where "n" is an integer. To measure the phase change through the test component, the position of the reference minimum is restored to its original position by adjustment of the short circuit. This condition may be expressed by:

$$\text{Arg } b_1/a_1\Big|_f = \text{Arg } b_1/a_1\Big|_i$$

where "f" and "i" represent final and initial values, respectively.

Now the scattering relations for a 2-port device are:

$$b_1 = S_{11}a_1 + S_{12}a_2 \qquad \cdots\cdots ①$$

$$b_2 = S_{21}a_1 + S_{22}a_2 \qquad \cdots\cdots ②$$

From ① $$b_1/a_1 = S_{11} + S_{12}a_2/a_1 \qquad \cdots\cdots ①a$$

From ② $$b_2/a_1 = S_{21} + S_{22}a_2/a_1$$

$$\frac{b_2}{a_2}\cdot\frac{a_2}{a_1} = S_{21} + S_{22}\frac{a_2}{a_1}$$

But $b_2/a_2 = \frac{1}{\rho_s}$, where ρ_s is the reflection coefficient of the short.

$$\therefore \frac{a_2}{a_1}\left[\frac{1}{\rho_s} - S_{22}\right] = S_{21}$$

Substituting for a_2/a_1 in equation (1a)

$$\therefore \frac{b_1}{a_1} = \rho_1 = S_{11} + S_{12}\left[\frac{S_{21}}{\frac{1}{\rho_s} - S_{22}}\right]$$

For a reciprocal device, $S_{12} = S_{21}$.

$$\therefore \rho_1 = S_{11} + \frac{S_{12}^2 \rho_s}{1 - S_{22}\rho_s}$$

Now the balance condition may be represented as:

$$\text{Arg}\left[S_{11} + \frac{S_{12}^2 \rho_s}{1 - S_{22}\rho_s}\right]_f = \text{Arg}\left[S_{11} + \frac{S_{12}^2 \rho_s}{1 - S_{22}\rho_s}\right]_i$$

or

$$\text{Arg}\left[S_{11} + \frac{S_{21}^2 \rho_s (1 + S_{22}\rho_s)}{1 - S_{22}^2 \rho_s^2}\right]_f = \text{Arg}\left[S_{11} + \frac{S_{21}^2 \rho_s (1 + S_{22}\rho_s)}{1 - S_{22}^2 \rho_s^2}\right]_i$$

Now for VSWR's < 2.0, $|S_{22}^2 \rho_s^2| << 1.0$

$$\therefore \text{Arg}\left[S_{11} + S_{21}^2 \rho_s + S_{21}^2 S_{22} \rho_s^2\right]_f = \text{Arg}\left[S_{11} + S_{21}^2 \rho_s + S_{21}^2 S_{22} \rho_s^2\right]_i$$

A graphical representation of the adjustment conditions for the general case is given in figure AII.2.

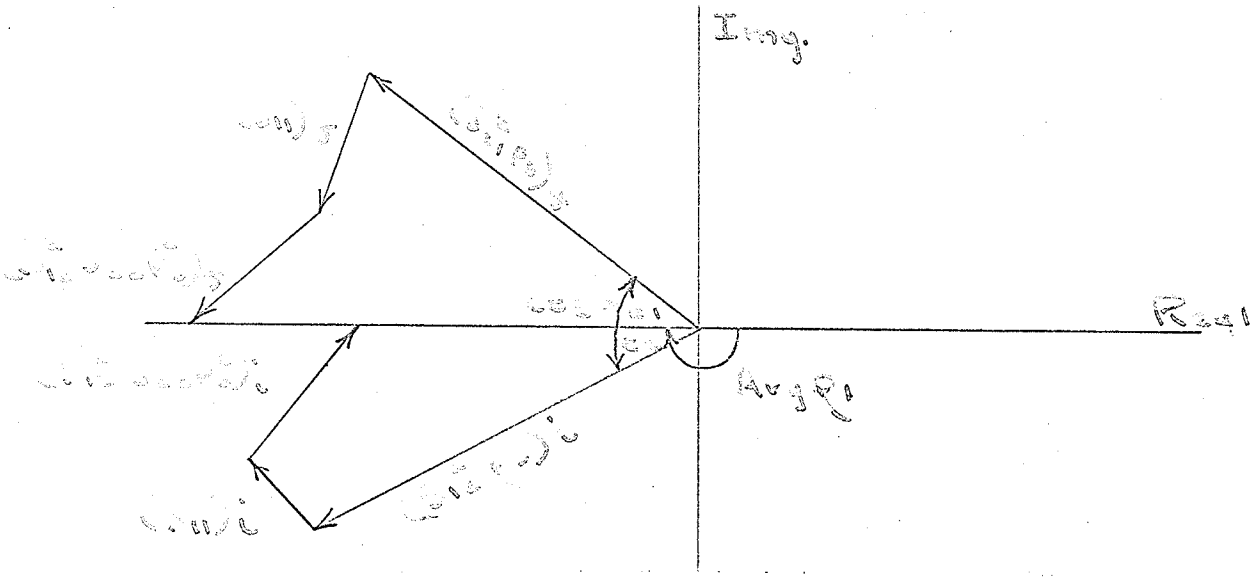

Figure AII.2

The measured variation of phase shift is based on the assumption that $S_{11} = S_{22} = 0$ and that the arguments of $(S_{21}^2 \rho_s)_f$ and $(S_{21}^2 \rho_s)_i$ are equal.

$$\text{i.e.} \quad \text{Arg}\left[S_{21}^2 \rho_s\right]_f = \text{Arg}\left[S_{21}^2 \rho_s\right]_i$$

$$\left[2\,\text{Arg}\, S_{21} + \text{Arg}\, \rho_s\right]_f = \left[2\,\text{Arg}\, S_{21} + \text{Arg}\, \rho_s\right]_i$$

$$\left[\text{Arg}\, S_{21}\right]_f - \left[\text{Arg}\, S_{21}\right]_i = \tfrac{1}{2}\left[\text{Arg}\, \rho_s\right]_i - \tfrac{1}{2}\left[\text{Arg}\, \rho_s\right]_f$$

This result states that the change in phase shift through the test component is equal to one half the change in phase of the reflection coefficient of the short circuit. This is the relation that was used to calculate the phase shift from the measured data. It can be seen that if $S_{11} = S_{22} \neq 0$,[a] this relation introduces an error into the calculated values of phase shift. Denoting this error by ϵ_e, then:

$$\left[\text{Arg}\, S_{21}\right]_f - \left[\text{Arg}\, S_{21}\right]_i - \tfrac{1}{2}\left[\text{Arg}\, \rho_s\right]_i + \tfrac{1}{2}\left[\text{Arg}\, \rho_s\right]_f = \epsilon_e$$

or

$$\text{Arg}\left[S_{21}^2 \rho_s\right]_f - \text{Arg}\left[S_{21}^2 \rho_s\right]_i = 2\epsilon_e$$

Referring to figure AII.2, it is seen that the difference between these arguments is $\epsilon_1 + \epsilon_2$

$$\therefore \epsilon_e = \frac{\epsilon_1 + \epsilon_2}{2}$$

The largest possible value of ϵ_1 occurs when S_{11} and $S_{12}^2 S_{22} \rho_s^2$ are collinear and perpendicular to ρ_1.

$$\therefore \text{Maximum } \epsilon_1 = \sin^{-1}\left[\frac{|S_{11}| + |S_{21}^2 S_{22} \rho_s^2|}{|S_{21}^2 \rho_s|}\right]_f$$

---

[a] For a lossless device, S_{11} always equals S_{22}.[24] In Chapter III, the VSWR was found to be reciprocal and hence $S_{11} = S_{22}$.

Similarly, maximum $\epsilon_2 = \sin^{-1}\left[\frac{|S_{11}| + |S_{21}^2 S_{22} e_s^2|}{|S_{21}^2 e_s|}\right]_i$

To simplify these expressions, the assumption $|S_{21}| = 1$ is made. This implies a lossless device. Also, for a perfectly reflecting short, $|e_s| = 1$.

$$\therefore \text{Max. } \epsilon_1 = \sin^{-1}[|S_{11}| + |S_{22}|]_f$$

$$\text{Max. } \epsilon_2 = \sin^{-1}[|S_{11}| + |S_{22}|]_i$$

Now for a lossless, bilateral device $|S_{11}| = |S_{22}|$

$$\therefore \text{Max. } \epsilon_e = (\sin^{-1}[2|S_{11}|]_f + \sin^{-1}[2|S_{11}|]_i)/2$$

This is the maximum possible error in one measurement of phase shift due to mismatch alone.

Now $|S_{11}| = |e_1|$ with port 2 matched.

$$\therefore |S_{11}| = \frac{\sigma_{11} - 1}{\sigma_{11} + 1}$$

From the VSWR data collected on each phase shift trial, the maximum error was, therefore, easily calculable.